Citation for the published paper:

[Couturier, Christine Stephanie; Stecyk, Jonathan Anthony William; Ellefsen, Stian; Sandvik, Guro Katrine; Milton, Sarah L.; Prentice, Howard M.; Nilsson, Göran Erik. (2019). The expression of genes involved in excitatory and inhibitory neurotransmission in turtle (Trachemys scripta) brain during anoxic submergence at 21°C and 5°C reveals the importance of cold as a preparatory cue for anoxia survival. ***Comparative Biochemistry and Physiology - Part D:Genomics and Proteomics*****. 30, 55-70]**

[DOI: 10.1016/j.cbd.2018.12.010]

The expression of genes involved in excitatory and inhibitory neurotransmission in turtle (*Trachemys scripta*) brain during anoxic submergence at 21°C and 5°C reveals the importance of cold as a preparatory cue for anoxia survival

Christine S. Couturier[1,6,*,§], Jonathan A. W. Stecyk[1,6,§], Stian Ellefsen[2,3], Guro K. Sandvik[1], Sarah L. Milton[4], Howard M. Prentice[5] and Göran E. Nilsson[1]

[1]*Programme for Physiology and Neurobiology, Department of Molecular Biosciences, University of Oslo, Norway*

[2]*Inland Norway University of Applied Sciences, Lillehammer, Norway*

[3]*Innlandet Hospital Trust, Brumunddal, Norway*

[4]*Department of Biological Sciences, Florida Atlantic University, Boca Raton, Florida, USA*

[5]*Department of Biomedical Sciences, Florida Atlantic University, Boca Raton, Florida, USA*

[6]*Department of Biological Sciences, University of Alaska Anchorage, Alaska, USA*

*Author to whom correspondence should be addressed. Email: cscouturier@alaska.edu

§ C. S. Couturier and J. A. W. Stecyk contributed equally to this work.

Abstract

We investigated if transcriptional responses are consistent with the arrest of synaptic activity in the anoxic turtle (*Trachemys scripta*) brain. Thirty-nine genes of key receptors, transporters, enzymes and regulatory proteins of inhibitory and excitatory neurotransmission were partially cloned and their expression in telencephalon of 21°C- and 5°C-acclimated normoxic, anoxic (24 h at 21°C; 1 and 14 days at 5°C) and reoxygenated (24 h at 21°C; 13 days at 5°C) turtles quantified by real-time RT-PCR. Gene expression was largely sustained with anoxia at 21°C and 5°C. However, the changes in gene expression that did occur were congruous with the decline in glutamatergic activity and the increase in GABAergic activity observed at cellular and whole organism levels. Moreover, at 21°C, the alterations in gene expression with anoxia induced a distinct gene expression pattern compared to normoxia and reoxygenation. Strikingly, acclimation from 21°C to 5°C in normoxia effectuated substantial transcriptional responses. Most prominently, 56% of the excitatory neurotransmission genes were down-regulated, including most of the ones encoding the subunits composing excitatory N-methyl-D-aspartate (NMDA) and 3-hydroxy-5-methyl-4-isoxazole propionate (AMPA) glutamate receptors. By contrast, only 26% of the inhibitory neurotransmission genes were down-regulated. Consequently, the gene expression pattern of 5°C normoxic turtles was statistically distinct compared to that of 21°C normoxic turtles. Overall, this study highlights that key transcriptional responses are consonant with the synaptic arrest that occurs in the anoxic turtle brain. In addition, the findings reveal that transcriptional remodelling induced by decreased temperature may serve to precondition the turtle brain for winter anoxia.

Keywords: GABA, gene expression, glutamate, mRNA, reoxygenation, synaptic arrest, telencephalon, temperature

Introduction

Most vertebrates, including mammals, are unable to survive more than a few minutes of anoxia because the energy demand of critical tissues such as the brain and heart cannot be sustained by anaerobic ATP production. By contrast, a few vertebrate species, such as the western painted turtle (*Chrysmemys picta*) and the red-eared slider turtle (*Trachemys scripta*), are able to survive prolonged periods of anoxia. At warm acclimation temperatures (20-25°C), these turtles successfully tolerate hours to days of anoxia, depending on species (Ultsch, 1985; Ultsch, 2006; Warren et al., 2006). To survive such harsh conditions, the turtles enter a severe metabolic depression. For example, whole animal metabolic rate of *C. picta* during anoxia at 20-24°C is 15-18% of that of normoxic, warm-acclimated turtles (Hammer et al., 2001; Jackson, 1968). The metabolic depression serves to balance ATP supply and demand when glycolytic fermentation is the only source of energy. It also spares the glycogen stores that are relied upon for the anaerobic production of ATP and slows the accumulation of acid metabolic end-products, which are buffered by the shell and the bones (Jackson, 2000a).

The reduction in turtle whole animal metabolic rate during anoxia exposure stems from reductions in energy demand in tissues. In 21-22°C-acclimated *T. scripta* exposed to 6 h of anoxic submergence, systemic cardiac power output, which reflects cardiac ATP demand, is 4.0- to 6.6-fold less than in normoxia (Hicks and Farrell, 2000; Stecyk et al., 2004). Similarly, in brain of warm-acclimated anoxic *T. scripta*, ATP turnover is reduced by 70-80% during 120 min of N_2 respiration, as suggested by levels of lactate production (Lutz et al., 1984). The reduction in brain ATP demand occurs due to the coordinated suppression of metabolic processes, including a cessation of protein synthesis after 1 h of anoxia at 23°C (Fraser et al., 2001) and a 30%-50% reduction of Na^+-K^+-ATPase activity after 24 h of anoxia at 20°C (Hylland et al., 1997; Stecyk et al., 2017). Additionally, at the level of the synapse, brain ATP demand is curtailed by key regulatory events that serve to limit excitatory neurotransmission, but activate inhibitory neurotransmission, a phenomenon termed ‘synaptic arrest’ (reviewed by Buck and Pamenter, 2018). Briefly, the release of the excitatory neurotransmitter glutamate is decreased to 30% of normoxic control values in *T. scripta* after 5 h of anoxia at 25°C (Thompson et al., 2007), and in *C. picta*, glutamate receptors, such as 3-hydroxy-5-methyl-4-isoxazole propionate (AMPA)

receptors (AMPARs) show a 50-60% reduction in AMPAR evoked peak current after 40 min of anoxic perfusion at 22°C (Pamenter et al., 2008b; Zivkovic and Buck, 2010). Also in *C. picta*, the opening probability and current amplitude of other glutamate receptors, the N-methyl-D-aspartate (NMDA) receptors (NMDARs), is reduced by 50–65% in neurons of the cerebrocortex within 1 to 60 min of anoxic perfusion at room temperature (Bickler et al., 2000; Buck and Bickler, 1998; Pamenter et al., 2008a). Simultaneously, massive amounts of the inhibitory neurotransmitter γ-aminobutyric acid (GABA) are released in the turtle brain, reaching 90-fold the level measured in normoxia after 4 h of anoxia at 25°C in *T. scripta* (Nilsson and Lutz, 1991). As demonstrated in *C. picta* cortical neurons, GABA suppresses spontaneous electrical activity via an increase in $GABA_A$ receptor-mediated postsynaptic activity and Cl^- conductance, which dampens excitatory potentials via shunting inhibition (Pamenter et al., 2011). GABA also decreases postsynaptic activity via $GABA_B$ receptor-mediated inhibition of presynaptic glutamate release (Pamenter et al., 2011). In addition, the density of the inhibitory $GABA_A$ receptor is increased in *T. scripta* by 30% following 24 h of anoxia at 25°C (Lutz and Leone-Kabler, 1995). Combined, the reduction of glutamate, the massive increase in GABA and the associated physiological responses lead to a decrease in excitatory glutamatergic receptor currents and an increase in inhibitory GABAergic receptor currents, which result in an overall decrease in neurotransmission. Consequently, nearly all nervous activity is suppressed in anoxia, leading the turtle into a comatose-like state.

While the ability of *T. scripta* and *C. picta* to survive anoxia at warm temperatures is impressive, their anoxia-tolerance at the cold temperatures (3-5°C) of the ice-covered ponds in which they overwinter is even more remarkable, extending to weeks to months, depending on species (Ultsch, 1985; Ultsch, 2006; Warren et al., 2006). Like at warm temperature, anoxia survival at cold temperature is aided by physiological changes that slow tissue energy demand, and therefore whole-animal metabolic rate. However, the reductions are quantitatively greater in cold, anoxic turtles compared to warm, anoxic turtles. In particular, whole-animal metabolic rate of *C. picta* is reduced to less than 90% of the cold, normoxic rate following 12 weeks of anoxic submergence at 3°C (Hammer et al., 2001; Jackson, 1968), systemic cardiac power output of 5°C-acclimated *T. scripta* is 7- to 20-fold less than in normoxia after 12-21 d of anoxic submergence (Hicks and Farrell, 2000;

Stecyk et al., 2004) and *T. scripta* brain Na^+-K^+-ATPase activity is suppressed by 50% after 14 days of anoxic submergence at 5°C (Hylland et al., 1997; Stecyk et al., 2017). The observed suppression for Na^+-K^+-ATPase activity with cold-temperature anoxia in *T. scripta* is quantitatively in-line with the 40% reduction of NMDA receptor activity in *C. picta* cerebrocortex after 6 weeks of anoxia at 2–3 °C (Bickler, 1998), as well as the 60% reduction in the abundance of the obligatory NMDAR subunit GluN1 in cerebrocortex of *C. picta* remaining anoxic at 3°C for 3-21 days (Bickler et al., 2000). However, whether prolonged anoxia exposure at cold temperature is also associated with regulatory events that serve to activate inhibitory neurotransmission in the turtle brain, namely an increase in inhibitory GABAergic receptor currents, remains unknown.

In addition to anoxia-induced responses, acclimation to low temperature is critical for extending anoxia survival time in the ectothermic champions of anoxia tolerance, including the turtles, crucian carp (*Carassius carassius*) and goldfish (*Carassius auratus*). Cold acclimation primes their physiological processes for prolonged anoxia survival by inducing whole-body metabolic depression (Hogg et al., 2014; Jackson and Ultsch, 2010; Ultsch, 1985), reduced cardiac function (Hicks and Farrell, 2000; Jackson and Ultsch, 2010; Stecyk, 2017; Stecyk et al., 2012; Stecyk et al., 2007; Stensløkken et al., 2010; Tikkanen et al., 2017; Vornanen et al., 2009) or brain function remodelling (Hogg et al., 2014; Stecyk et al., 2012; Stensløkken et al., 2010). Importantly, during cold acclimation, these organisms actively suppress biological rate processes beyond the direct depression imposed by the reduced kinetic energy of molecules at lowered temperature. The phenomenon, termed inverse thermal compensation, is reflected in Q_{10} values greater than 2 for a number of physiological parameters and is believed to signify the priming of physiological processes to conserve ATP as a preparation for winter anoxia (Hochachka, 1986; Jackson, 2000b; Stecyk et al., 2008). Nevertheless, while studies on turtle whole animal and cardiac metabolic rate have factored in the effect of decreased temperature, most previous investigations of the cellular anoxia tolerance of the turtle brain have not. Consequently, it remains unknown how excitatory and inhibitory neurotransmission in the turtle brain are affected by acclimation to low temperature in normoxia.

The overarching aim of the present study was to investigate if altered transcription is a mechanism through which excitatory neurotransmission is limited, but inhibitory neurotransmission is increased in the anoxic turtle brain. Indeed, a fine-tuned regulation of gene expression is a vital aspect of anoxia survival and metabolic depression in *T. scripta* liver and skeletal muscle (Bansal et al., 2016; Biggar and Storey, 2011, 2015; Greenway and Storey, 2000; Krivoruchko and Storey, 2010a, 2013; Wijenayake et al., 2018; Zhang et al., 2013), and the contribution of altered transcription to synaptic arrest is supported by the reversible decrease of voltage-dependent K^+ channel transcription in *T. scripta* brain during 4 h of anoxia at 25°C (Prentice et al., 2003). Moreover, in crucian carp, which like the turtle exhibits a profound anoxia tolerance, although with a functional (active) brain (Lutz and Nilsson, 1997; Nilsson, 2001), the expression of critical genes involved in excitatory and GABAergic neurotransmission is altered by prolonged anoxia exposure (7 days at 9 or 12°C) amongst a background of a largely sustained level of gene expression (Ellefsen et al., 2008a; Ellefsen et al., 2009). To this end, we partially cloned 39 genes of key receptors, transporters, enzymes and regulatory proteins involved in inhibitory and excitatory neurotransmission (Table 1) and quantified their expression in telencephalon of 21°C- and 5°C-acclimated normoxic and anoxic (24 h at 21°C; 1 day and 14 days at 5°C) *T. scripta* using real-time RT-PCR. 21°C-acclimated turtles were studied to allow comparison of changes in gene expression to the existing body of knowledge on cellular anoxia tolerance of the turtle brain at high temperature. 5°C-acclimated turtles were studied to address the information gap on the cellular mechanisms of brain anoxia tolerance in turtles at cold temperature. For both acclimation temperatures, we hypothesized that target gene expression would be down-regulated in anoxia in-line with the massive depression of whole-animal and brain metabolic rate displayed by anoxic turtles. However, we also predicted that the effects of anoxia on gene expression would be differential. We surmised that the target genes would show varying degrees of down-regulation reflective of the functional role of the protein a target gene encodes for (i.e., excitatory or inhibitory neurotransmission). Additionally, to provide novel insight into how excitatory and inhibitory neurotransmission in the turtle brain are affected by acclimation to low temperature, we investigated the effects of acclimation to low temperature in normoxia (8 weeks). We hypothesized that acclimation to low temperature would induce

changes in gene expression reflective of a priming of the brain for energy conservation. Finally, we investigated the effect of reoxygenation (24 h at 21°C; 13 days at 5°C) to determine if the changes in gene expression that occurred with anoxia exposure recovered to normoxic levels. In 8°C-acclimated crucian carp, the changes in gene expression that occurred in brain with a 7-day anoxia exposure at 9 or 12°C largely failed to recover to pre-exposure levels within 7 days of reoxygenation (Ellefsen et al., 2008a; Ellefsen et al., 2009). The lack of recovery was proposed to reflect that anoxia exposure at low temperature serves as a cue for further and longer anoxic exposures. Indeed, in nature, prolonged winter anoxia is likely preceded by several shorter bouts of hypoxia and anoxia. We thus hypothesized that similar findings would be found for the 5°C-acclimated turtles, but not those acclimated to 21°C, where prolonged anoxia exposure is unnatural and reoxygenation is more analogous to recovery in species where anoxia is a rare or pathological phenomenon.

To assess excitatory neurotransmission (Table 1), we measured the gene expression of glutamate receptor subunits GluN1, GuN2A-D and GluN3A for NMDARs, GluA1-4 for AMPARs, as well as transmembrane excitatory amino acid transporters (EAAT2 and 3) that remove glutamate from the synapse to end the excitatory signal. We also measured the gene expression of key proteins involved in NMDAR-mediated neuroplasticity, including activity-regulated cytoskeleton-associated protein (ARC), brain-derived neurotrophic factor (BDNF) and its receptor tropomyosin receptor kinase B (TrkB) and cAMP responsive element binding protein (CREB1) that stimulates transcription. To assess inhibitory neurotransmission (Table 1), we measured the gene expression of $GABA_A$ receptors (subunits α1-6, β2-3, δ, γ1-3), $GABA_B$ receptors (subunits 1 and 2), GABA receptor-associated protein (GABARAP) that clusters GABA receptors by mediating interaction with the cytoskeleton, plasma membrane GABA transporters (GAT1-3) that mediate the uptake of GABA from the extracellular to the intracellular space, and two isoforms of L-glutamic acid decarboxylase (GAD_{65} and GAD_{67}) that catalyze the decarboxylation of glutamate to GABA. We also measured the gene expression of the vesicular GABA transporter (vGAT), which is responsible for the uptake and storage of GABA by synaptic vesicles in the central nervous system, as well as the gene expression of the K-Cl co-transporter (KCC2) and the Na-K-Cl

cotransporter 1 (NKCC1), which together govern the impact (i.e., excitatory or inhibitory) of $GABA_A$ receptor activation.

T. scripta was chosen as the study species for three reasons. First, even though the anoxia survival time of *T. scripta* is less than *C. picta*, its survival time at both high and low temperature greatly surpasses that of almost all vertebrates. Therefore, the remarkable anoxia resilience of *T. scripta* makes it an exciting model organism to study. Second, as summarized above, prior studies at the cellular and whole animal level have established physiological baselines for the effects of anoxia, and importantly cold acclimation, on *T. scripta* brain and cardiovascular function. Finally, we wanted to provide a comparative, rather than duplicative, study to the recent transcriptomic investigation of the effects anoxia exposure (24 h anoxia at 19°C) on gene expression in *C. picta* telencephalon (Keenan et al., 2015).

Materials and Methods

Experimental animals and ethical approval

Turtles of both sexes (0.51 kg ± 0.11 kg, mean ± S.D.; N =59) were obtained from a commercial supplier (Nasco, Fort Atkinson, WI) and air-freighted to the University of Oslo. The 22 turtles studied at 21ºC were held at room temperature (21°C ± 1°C; 12 h:12 h L:D photoperiod) for 8 weeks in aquaria with free access to basking platforms. They were fed several times a week with commercial turtle food pellets. The other 37 turtles were kept in aquaria within a temperature-controlled room at 5ºC ± 1°C (12 h:12 h L:D photoperiod) for 8 weeks to ensure proper acclimation (Hicks and Farrell, 2000). The exposure to 5ºC occurred during autumn and the turtles were fasted during the entire period. All animals appeared healthy and experimental protocols were approved by the Norwegian Animal Research Authority and performed in accordance with relevant guidelines and regulations.

Experimental design

Turtles were sampled from one of three exposure conditions: 1) normoxia (control normoxic groups); 2) after periods of anoxia exposure; and 3) following reoxygenation after a prior anoxia exposure, as detailed in Table 2. At 21ºC, the control normoxic exposure lasted 1 day (21N1), the anoxia exposure 1 day (21A1) and the reoxygenation regime 1 day following a 1-day anoxia exposure (21A1N1). At 5ºC, the control normoxic exposure lasted 14 days (5N14), the anoxia exposures 1 day (5A1) and 14 days (5A14), and the reoxygenation regime 13 days following a 14 day-anoxia exposure (5A14N13). The exposure times were chosen to be physiologically relevant and consistent with previous studies examining the anoxic turtle brain at high and low temperature (Bickler, 1998; Bickler et al., 2000; Hylland et al., 1997; Keenan et al., 2015; Kesaraju et al., 2009; Krivoruchko and Storey, 2010b; Lutz and Leone-Kabler, 1995; Stecyk et al., 2012; Stecyk et al., 2017; Warren and Jackson, 2007). At 5ºC, after 1 day in anoxia, turtles are in a transitional period and reach a new physiological steady-state after about 2 weeks. At 21 ºC, *T. scripta* cannot survive beyond 24 h in anoxia and therefore, turtles were sampled after only 1 day of anoxia exposure. Normoxia and reoxygenation exposures were time-matched to the anoxia exposures.

At 21ºC, the control normoxia, anoxia and reoxygenation exposures were performed on individual turtles placed into water-containing plastic chambers for at least 24 h prior to experimental manipulation. Anoxic conditions were achieved by sealing the housing chamber with a tight-fitting lid, completely filling it with water that was continuously gassed with N_2 and suspending a metal mesh below the surface of the water to deny the turtle access to the surface. For the 21ºC control normoxic turtles, the water level remained low enough to allow the turtle air access and the water gassed with room air at a similar flow rate as the N_2-gassed turtles. At 5ºC, the control normoxia, anoxia and reoxygenation exposures were performed on groups of turtles placed into large aquaria. Like at 21ºC, for the anoxia exposures at 5°C, the aquaria were fitted with a tight lid, a mesh suspended below the water line so that the turtles could not surface, and the water continuously gassed with N_2. In all instances, the turtles were unrestrained and were free to move within the experimental chambers. All turtles survived the experimental treatments. Water temperature and oxygen concentration were monitored

with a galvanometric oxygen electrode (Oxi 323, WTW, Weilheim, Germany). Water with no detectable oxygen (<0.1 mg O_2 l^{-1}; = 0.16 kPa) was considered anoxic.

Tissue sampling

At each sampling time, turtles were quickly removed from the exposure tank and killed by decapitation. Within 30 s of the initiation of animal handling, the brain was removed, the telencephalon dissected, snap-frozen in liquid N_2 and stored at -80ºC.

RNA extraction

Total RNA was extracted from untreated turtle telencephalon using TRIzol® reagent (Invitrogen, Carlsbad, CA, USA). The extractions were performed in accordance with the protocol previously outlined by Ellefsen et al. (2008b) and Stecyk et al. (2012) in which an external RNA control gene is added to the tissue on a per unit weight basis to provide an external reference for real-time RT-PCR quantification. Briefly, frozen tissue was weighed on a precision balance and immersed in 15 µl TRIzol per mg tissue. Then, 100 pg per mg tissue of the external RNA control gene (mw2060; corresponding to 9 x 10^7 copies per mg tissue) was added and the tissue/TRIzol/mw2060 mixture homogenized for 1 min using a T-25 Basic homogenizer (IKA Works, Inc., Wilmington, NC, USA). Here, it should be noted that mw2060 was synthesized immediately prior to the RNA extraction to avoid potential degradation. Samples were then chilled on ice, vortexed, incubated at room temperature for 15 min and vortexed again. For tissue samples greater than 66 mg, 1000 µl of the homogenate (corresponding to 65.8 mg of tissue) was transferred to an Eppendorf tube, 187.5 µl of chloroform added, the mixture incubated at room temperature for 3 min, vortexed, centrifuged at 10000 **g** for 15 min at 4ºC and placed on ice. Four-hundred µl of the upper aqueous phase was then transferred to a new Eppendorf tube, 400 µl of ice-cold isopropanol added, the mixture vortexed, incubated at -20ºC for 10 min, incubated at room temperature for 10 min and centrifuged at 11500 **g** for 10 min at 4ºC. The supernatant was then discarded, and the pellet washed two times with ice-cold 75% ethanol. Each ethanol wash was followed by centrifugation at 11500 **g** for

10 min at 4ºC. After the last ethanol wash, the pellet was air-dried and eluted in 30 µl of nuclease free water (Ambion, Austin, TX, USA). The mixture was then incubated at 65ºC for 5 min to ensure the pellet was completely dissolved and stored at -80ºC. For tissue samples less than 66 mg, 500 µl of the tissue/TRIzol/mw2060 homogenate (corresponding to 32.9 mg of tissue) was processed with all above stated volumes reduced proportionately.

Care was taken to avoid systematic errors introduced by sample processing during RNA extraction. All samples were handled without intermission and in a systematic, yet random order. Samples were processed in groups, wherein each group represented each of the seven temperature and oxygen exposure regimes. The samples within each group were processed at random. Similar procedures were also employed for cDNA synthesis.

cDNA synthesis

The quality of the extracted RNA was assessed in a randomly selected subset of samples on a 2100 Bioanalyzer (Agilent Technologies, Palo Alto, CA, USA) and the concentration of total RNA in every sample determined using a NanoDrop® ND-1000 UV-Vis Spectrophotometer (NanoDrop Technologies, Rockland, DE, USA). One µg of total RNA from each sample was treated with DNase I (DNA-free; Invitrogen, Carlsbad, CA, USA) and subsequently reverse transcribed using Random Hexamers (50 ng/µl) and Superscript III (both from Invitrogen, Carlsbad, CA, USA) in reaction volumes of 20 µl and in accordance with the manufacturer's protocol. cDNA solutions were diluted 1:30 with nuclease free water and stored at -20ºC. Duplicate cDNA syntheses were performed on all RNA samples.

Cloning of the genes

The sequences of the 39 genes of interest were obtained by cloning, using PCR primers recognizing gene regions conserved among vertebrate species. These regions were located using GeneDoc (version 2.7.00,

http://www.psc.edu/biomed/genedoc/) and ClustalX (version 2.00; Thompson et al., 1997), while primers were designed using Primer3 (Rozen and Skaletsky, 2000).

PCR was performed on a mixture of 1:30 diluted cDNA from warm, cold, normoxic and anoxic turtle telencephalon using Platinum®*Taq* DNA Polymerase (Invitrogen, Carlsbad, CA, USA; 94°C for 10 min, 94°C for 30 sec, 48°C for 1 min, 72°C for 1 min, repeat steps 2-4 44x, 72°C for 10 min, hold 4°C). Resulting dsDNA fragments were ligated into pGEM®-T Easy Vector System I (Promega, Madison, WI, USA). Ligation reactions were transformed into $CaCl_2$-competent cells (TOP10 F'; Invitrogen, Carlsbad, CA, USA), whereupon positive colonies were checked for inserts of correct size via agarose gel electrophoresis. PCR products from a minimum of eight colonies were sequenced using T7 primers (ABI-lab, University of Oslo, Oslo, Norway). All procedures were carried out according to the manufacturer's protocol. The resulting turtle sequences were submitted to the GenBank sequence database (BankIt-NCBI-NIH https://www.ncbi.nlm.nih.gov/BankIt) and the accession numbers are listed in Table 2.

Real-time RT-PCR protocol and primer design

Real-time RT-PCR was performed using Lightcycler® 480 (Roche Diagnostics, Basel, Switzerland). All real-time RT-PCR reactions were performed in a reaction volume of 10 µl that contained 5 µl of Lightcycler® 480 SYBR Green I Master (Roche Diagnostics, Basel, Switzerland), 3 µl of 1:30 diluted cDNA as the template, 1 µl of 5 mM gene-specific forward primer and 1 µl of 5 mM gene-specific reverse primer (i.e., final primer concentrations of 1 mM). The following real-time RT-PCR program was used: 95°C for 10 min, 95°C for 10 sec, 60°C for 10 sec, 72°C for 13 sec, repeat steps 2-4 42x. Two real-time RT-PCR reactions were performed on each gene for each cDNA synthesis. The replicates were conducted on different plates and days. Since two cDNA syntheses were performed for each total RNA sample, a total of four real-time RT-PCR reactions were performed on each gene for each sample of total RNA.

All real-time RT-PCR primer pairs were designed from the cloned sequences using Primer3 (Rozen and Skaletsky, 2000). Forward and reverse primers were targeted to either side of an exon-exon overlap as a further precaution against amplifying genomic DNA (i.e., in addition to the extraction of total RNA and DNAse treatment). Amplification of the desired cDNA species by the primer pairs was verified by melting curve analyses (Lightcycler® 480 software) and cloning and sequencing of all primer pair products (performed as described above for *Cloning of the genes*). Primer sequences, efficiencies and average quantification cycle (Cq; i.e., "crossing point" or "threshold cycle") values obtained for the primer pairs are summarized in Table 2. In order to find primers that worked well with the outlined real-time RT-PCR protocol (primer concentration of 1 mM and annealing temperature of 60°C), a minimum of four primer pairs were tested for each gene. The primer pairs that displayed distinct melting curves, the highest efficiency (calculated as described below for *Real-time RT-PCR analyses*) and the lowest Cq values were chosen. This was done as an alternative to primer concentration/annealing temperature optimization. All procedures were carried out according to manufacturer's protocol.

Real-time RT-PCR analyses

Cq values were obtained for each reaction using the Lightcycler® 480 software and were defined according to the second derivative maximum (Luu-The et al., 2005). Priming efficiencies were calculated for each real-time RT-PCR reaction using LinRegPCR software (Ruijter et al., 2009), but in the final calculations, average priming efficiencies (E_{mean}) were used, calculated separately for each primer pair from all real-time RT-PCR reactions (Table 2; Cikos et al., 2007). Then, E_{mean}^{Cq} was calculated for every reaction, as well as the ratio (R1) between ${}_{mw2060}E_{mean}^{Cq}$ and ${}_{Tar}E_{mean}^{Cq}$ in order to normalize target gene mRNA expression to the expression of the external RNA control mw2060 (where Tar = target gene, E = priming efficiency and Cq = quantification cycle).

To compare the expression of each gene among the different oxygen regimes for each temperature, the ratio R1 was referenced to the mean gene expression of the control normoxic turtles. Likewise, to compare the

313 effect of 5ºC acclimation on the expression of each gene, the ratio R1 at 5ºC in normoxia was referenced to the
314 mean gene expression in normoxia at 21ºC.
315
316 *Calculations and Statistical analyses*

317 Total telencephalon RNA content (ng RNA/mg tissue) was calculated from the concentration of total
318 RNA extracted per sample as determined using a NanoDrop® ND-1000 UV-Vis Spectrophotometer (see *cDNA*
319 *synthesis* above) and tissue mass. To place the expression of singular genes into the context of complementary
320 genes, gene-family profiling analysis was conducted for the sets of genes that share baseline properties and/or
321 fulfil similar physiological roles (Table 4; Ellefsen and Stenslokken, 2010). Specifically, for each gene family,
322 the relative abundance (i.e., profiling) of each family member was calculated as a percentage of overall gene-
323 family mRNA abundance within each exposure condition.
324 Statistical analyses were performed using JMP 8 (Aspire Software International, Ashburn, USA) to
325 evaluate whether the different oxygen and temperature regimes affected individual gene expression and gene-
326 family profiles, and PAST 3.22 (Hammer et al., 2001) to determine if the pattern of gene expression differed
327 among exposure conditions. One-way ANOVAs followed by a TukeyHSD *post hoc* test were used to determine
328 statistically significant effects of anoxia and reoxygenation on the log10 transformed (Hellemans and
329 Vandesompele, 2011) target gene expression at each acclimation temperature (Del Toro et al., 2003; Ellefsen et
330 al., 2008a; Ellefsen et al., 2009; Ellefsen and Stenslokken, 2010; Prentice et al., 2003; Stecyk et al., 2012;
331 Tikkanen et al., 2017; Wilson et al., 2013). Student's *t*-tests were used to assess the effect of acclimation
332 temperature on gene expression by comparing the log10 transformed (Hellemans and Vandesompele, 2011)
333 target gene expression of normoxic turtles at 21ºC and 5ºC . Gene-family profiles expressed as percentages
334 were arcsine-transformed prior to statistical analyses. A pairwise one-way permutational multivariate analysis
335 of variance (PERMANOVA) was used to determine statistically significant differences in the pattern of gene
336 expression among the seven exposure conditions. In all instances, significance was accepted when $P<0.05$.

Principle component analysis (PCA) was conducted to visualize gene expression patterns among the different oxygen and temperature regimes. Principle components were calculated using the Factoextra package (Kassambara, 2015) in R 3.5.1 (R Development Core Team, 2009). Corresponding factor maps were created to demonstrate the contribution of the response variables (i.e., the 39 gene targets) to the principle components.

Results

We successfully partially cloned all target genes we aimed to measure except for *Gabrb1* (encodes $GABA_A$ β1). Many primer pairs were designed to amplify a partial sequence of this gene, but *Gabrb1* expression might have been below detection levels.

Tissue total RNA content

Telencephalon total RNA content ranged between 632 ±182 and 773 ±95 ng mg^{-1} tissue and did not show any significant changes with acclimation temperature or oxygen availability (Table 1; Stecyk et al., 2012).

Effects of anoxia and reoxygenation at 21°C on individual gene expression and gene-family profiles

At 21°C, six genes showed a change in expression with oxygenation status (Table 3; Fig.1). For genes involved in excitatory neurotransmission, the expression of *Arc* (encodes ARC) doubled after one day in anoxia and returned to the control normoxic level after one day of reoxygenation. By contrast, expression of *Slc1a1* (encodes EAAT3), decreased by 24% in anoxia and returned to a level not statistically different than control normoxia upon reoxygenation. *Bdnf*, *Creb1* and *Gria1*, which encode BDNF, CREB1 and GluA1, respectively, showed an overcompensation with reoxygenation. *Bdnf* decreased by 34%, whereas *Creb1* and *Gria1* expression increased by 39% and 20%, respectively, compared to anoxic levels after 1 day of reoxygenation.

For genes involved in inhibitory neurotransmission, *Gabra5* (encodes $GABA_A$ α5) decreased by 41% in anoxia compared to normoxia (Fig. 2). Moreover, the proportion of $GABA_A$ α subunit mRNA varied with

oxygenation state (Table 4; Fig. 2). The relative abundance of *Gabra5* decreased by 29% after 1 day in anoxia compared to the control normoxic level, whereas the proportion of *Gabra2* (encodes $GABA_A$ α2) decreased by 15% with reoxygenation compared to anoxia.

Effects of anoxia and reoxygenation at 5 ℃ on individual gene expression and gene-family profiles

At 5°C, three genes exhibited a change in expression with oxygenation status (Table 5; Fig. 3). For genes involved in excitatory neurotransmission, only *Arc* was affected. Contrary to the response of *Arc* to 24 h of anoxia exposure at 21°C, *Arc* expression was reversibly decreased by 31% after 14 days of anoxia at 5°C. In addition, the gene-family profiles of the GluA subunits of AMPARs and the GluN subunits of NMDARs were modified by oxygenation state at 5°C (Table 4; Fig. 2). Within the GluA subunit gene family, the proportion of *Gria1* (encodes GluA1) increased by 31%, whereas the proportion of *Gria2* (encodes GluA2) decreased by 14% after reoxygenation compared to 14 days of anoxia. Within the GluN subunit gene family, the results of the ANOVA yielded significant differences among the exposure groups. However, no statistically significant differences among oxygenation state were revealed by the Tukey HSD *post-hoc* test.

For genes involved in inhibitory neurotransmission, the expression of *Gabarap* (encodes GABARAP) and *Gabrd* (encodes $GABA_A$ δ) was altered. *Gabarap* decreased by 31% after 1 day of anoxia, but then its expression settled at a level intermediate to control normoxia and 1 day of anoxia by 14 days of anoxia exposure, where it remained upon reoxygenation (Table 5; Fig. 3). *Gabrd* expression was unchanged by anoxia exposure, but it was decreased by 30% after reoxygenation compared to normoxia. Additionally, the relative expression of *Slc6a11* (encodes GAT3) within the GAT gene family decreased by 38% after 14 days of anoxia (Table 4; Fig. 2).

Effect of cold acclimation in normoxia on individual gene expression and gene-family profiles

Acclimation from 21°C to 5°C in normoxia lead to an altered expression of 15 genes (Fig. 4). None of the genes exhibited an increase in expression and sixty percent of the genes altered were those involved in

386 excitatory neurotransmission. For genes involved in excitatory neurotransmission, decreased expression was
387 found for *Creb1* (encodes CREB1, -29%), three of the four AMPAR subunits (*Gria2*, encodes GluA2, -28%;
388 *Gria3*, encodes GluA3, -22%; *Gria4*, encodes GluA4, -52%) and five NMDA receptor subunits (*Grin1*, encodes
389 GluN1, -36%; *Grin2a*, encodes GluN2A, -33%; *Grin2b*, encodes GluN2B, -40%; *Grin2d*, encodes
390 GluN2D, -28%; *Grin3a*, encodes GluN3A, -32%). Additionally, the proportion of *Gria2* and *Gria4* expression
391 within the GluA gene family was reduced by 6 and 43%, respectively, whereas the proportion of *Grin2d* within
392 the GluN2 gene family increased by 23% (Table 4; Fig. 2).
393 For genes involved in inhibitory neurotransmission, reduced gene expression was observed for three
394 $GABA_A$ subunits (*Gabra3*, encodes $GABA_A$ α3, -53%; *Gabra5*, encodes $GABA_A$ α5, -28%; *Gabra6*, encodes
395 $GABA_A$ α6, -66%), two GABA transporters (*Slc6a1*, encodes GAT1, -37%; *Slc6a13*, encodes GAT2, -59%)
396 and the Na-K-Cl cotransporter NKCC1 (*Slc12a2*, -33%) (Fig. 4). Combined, these changes led to decreased
397 proportions of *Gabra3* (encodes $GABA_A$ α3, -41%) and *Gabra6* (encodes $GABA_A$ α6, -57%) within $GABA_A$ α
398 subunit gene family, as well as decreased relative expression of *Slc6a13* (encodes GAT2, -49%), but increased
399 relative expression of *Slc6a11* (encodes GAT3, +63%) within the GAT gene family (Table 4; Fig.2).
400
401 *Effect of exposure condition on the pattern of gene expression*
402 The pairwise multivariate comparisons (i.e. PERMANOVA) and PCA analyses of target gene
403 expression among the seven exposure conditions revealed that the gene expression pattern of 21°C anoxic
404 turtles significantly separated from that of 21°C normoxic and reoxygenated turtles (Table 6; Fig. 5). By
405 contrast, gene expression pattern was not affected by oxygenation state at 5°C (Table 6; Fig. 5). However, the
406 substantial transcriptional responses induced by acclimation from 21°C to 5°C in normoxia resulted in cold-
407 acclimated turtles exhibiting a statistically distinct gene expression pattern compared to warm-acclimated turtles
408 (Table 6; Fig. 5)
409

Discussion

The overarching goal of the present study was to quantify the gene expression of key receptors, transporters, enzymes and regulatory proteins involved in excitatory and inhibitory neurotransmission in telencephalon of anoxia-tolerant red-eared slider turtles exposed to various oxygenation states (normoxia, anoxia and reoxygenation) at high and low acclimation temperature (21°C and 5°C). Our specific objective was to determine if alterations of gene expression evince the profound neuronal anoxia-tolerance of the species. Overall, our findings provide important insights into the role oxygenation state plays in precipitating transcriptional responses that may facilitate synaptic arrest, and thereby neuronal tolerance of anoxia in the turtle brain. Moreover, our findings emphasize the importance of cold acclimation in preparing the turtle brain for prolonged anoxia survival in winter.

Modification of gene expression by anoxia and reoxygenation

Few statistically significant differences in gene expression occurred with anoxia exposure and reoxygenation at high or low temperature. The finding, although contrary to our hypothesis, has a number of important implications. Primarily, it indicates that drastically altered brain gene expression on a global scale is not a molecular characteristic that differentiates the contrasting anoxia-survival strategies of the freshwater turtle and crucian carp. Correspondingly, only 19 of 13,236 mRNAs showed a greater than 2x difference (up or down) in expression in telencephalon of the *C. picta* exposed to 24 h of anoxia at 19°C: none of which were related to ion channels or synaptic transmission (Keenan et al., 2015). Secondly, the juxtaposition between relatively stable gene expression, but ceased protein synthesis (Fraser et al., 2001) in the anoxic *T. scripta* brain indicates that post-transcriptional, translational and/or post-translational modifications must be important control points in the fine-tuning of neuronal gene expression in anoxia. Thirdly, the finding suggests that mRNA turnover may be altered with anoxia exposure. A disruption of mRNA decay, rather than continuous transcription and subsequent degradation, could lead to the maintained gene expression observed in the anoxic turtle and crucian carp brain. Investigation into how mRNA turnover is modified in anoxia would be an

interesting avenue for future study, especially given that destabilization of mRNAs encoding for synaptic transmission proteins is associated with neurodegenerative diseases states in the mammalian brain (Alkallas et al., 2017). Finally, the finding implies that the changes in gene expression that did occur are key transcriptional responses despite their seemingly small magnitude, which ranged from a 70% decrease to a 100% increase.

At 21°C, the gene expression of ARC (*Arc*), EAAT3 (*Slc1a1*) and $GABA_A$ α5 (*Gabra5*) was altered by 1 day of anoxia exposure. Unlike most genes in this study, which exhibited a decreased expression with anoxia or acclimation to low temperature, the expression of *Arc* increased two-fold. *Arc* belongs to the immediate-early gene (IEG) family, which is rapidly activated and able to be transcribed even in the presence of protein synthesis inhibitors, indicating that the proteins required for their transcription are constitutively present in the cell (Bahrami and Drabløs, 2016). The IEG characteristic of *Arc* likely underlies its increased expression in anoxia at 21°C, when most protein synthesis is halted (Fraser et al., 2001). In mammals, ARC participates to the removal of GluA2-containing AMPARs from the synaptic membranes by accelerating endocytosis and reducing surface expression (Chowdhury et al., 2006), leading to a reduction of excitatory AMPAR-mediated synaptic transmission (Pamenter et al., 2008b; Rial Verde et al., 2006). In *T. scripta*, the GluA2-containing AMPAR appears to be the most prevalent type of AMPAR, when judged from the gene expression levels (Table 4; Fig. 2). Thus, when turtles experience anoxia without prior cold acclimation, ARC could participate to lower the expression of AMPAR subunits through its effects on AMPAR trafficking. However, the increased expression of *Arc* could also be a passive consequence of a transient increase in (dysregulated) electrical activity in the turtle brain following onset of anoxia at high temperatures. Indeed, the turtle brain is not set to handle abrupt incidents of anoxia at this high temperature, leading to possible uncontrolled electrical activity, in turn leading to increased *Arc* expression. The increased expression of *Arc* could then be seen as an indicator of the need for preparing for anoxia, i.e. the cold-induced changes in expression of excitatory ion channels in the cells in order to meet the anoxic challenge. The gene expression of the glutamate transporter EAAT3 (*Slc1a1*) was decreased by 24% with anoxia at 21°C, whereas the gene expression of the glutamate transporter EAAT2 (*Slc1a2*) was unchanged. In humans, EAAT3 is primarily found in neurons, dendrites and axon terminals (Holmseth et al.,

2012), whereas EAAT2 is mainly found in astroglial cells (Roberts et al., 2014), but low levels have also been found at synaptic sites in rodents (Furness et al., 2008). EAAT2 is responsible for most of the glutamate reuptake in the brain to limit excitatory neurotransmission (Suchak et al., 2003; Tanaka et al., 1997), and this could explain why EAAT2 gene expression did not change in anoxia. By comparison, EAAT3 gene expression represented only a quarter of the total EAAT gene family mRNA abundance. Among the 12 $GABA_AR$ subunit genes cloned in this study, *Gabra5* was the only one that showed a significant change in expression with oxygenation state (-41% with anoxia at 21°C). $GABA_AR$ are pentamers and the subunit composition of the receptor, particularly its alpha-subunit content, determines its pharmacological characteristics (Smith, 2001). Why $GABA_A$ α5 is the only subunit to show a significant decrease in gene expression in anoxia remains to be determined.

With reoxygenation at 21°C, the gene expression of BDNF (*Bdnf*), CREB1 (*Creb1*) and GluA1 (*Gria1*), was affected. BDNF activates postsynaptic cascades that increase ARC levels once it binds to TrkB (Giorgi et al., 2007). Thus, the 34% decrease of *Bdnf* from the anoxic level during reoxygenation correlates with the return of *Arc* to normoxic levels with reoxygenation. The 39% increased gene expression of the transcription factor CREB1 with reoxygenation at 21°C could point towards a general up-regulation of gene transcription at time-points beyond 24 h of reoxygenation. The 20% up-regulated *Gria1* may reflect unsilencing of synapses (Selcher et al., 2012).

With 14 days of anoxia at 5°C, the gene expression of ARC (*Arc*) and GADARAP (*Gadarap*) was affected. With subsequent 13 days of rexoygenation at 5°C, the gene expression of $GABA_A$ δ (*Gabrd*) was altered. Contrary to the increased *Arc* expression with anoxia exposure at high temperature, *Arc* showed a 31% decrease in expression after 14 days in anoxia at 5°C. Glutamatergic neurons in the brain express ARC in response to an increase in synaptic activity (Korb and Finkbeiner, 2011), but glutamatergic activity is reduced in anoxia (Pamenter et al., 2008b; Thompson et al., 2007), which could limit the expression of ARC. *Gabarap* showed a significant decrease the first day of anoxia, but then increased with subsequent exposure. GABARAP is known to cluster GABA receptors by mediating their interaction with the cytoskeleton, thereby inactivating

485 them (Wang et al., 1999). Therefore, the decreased expression of *Gabarap* at the onset of anoxia exposure (i.e.,
486 5A1) could serve to limit the inactivation of inhibitory GABA receptors. *Gabrd* showed a significant decrease
487 in expression during reoxygenation compared to normoxia. As with the other $GABA_AR$ subunits, $GABA_A$ δ
488 provides specific biochemical properties to the channel. It slows the rate of acute desensitization of GABA-
489 evoked current and the rate of recovery of GABA-evoked current (Saxena and Macdonald, 1994) to potentiate
490 the effects of GABA. Such effects are no longer needed when oxygen is restored.
491
492 *Modification of gene expression with cold temperature*
493 Compared to anoxia exposure at high and low temperature, considerably more changes in gene
494 expression occurred with acclimation from 21°C to 5°C in normoxia. Ultimately, the low temperature-induced
495 alterations in gene expression resulted in 5°C normoxic turtles having distinct gene expression pattern compared
496 to the 21°C normoxic turtles. This finding corroborates previous studies on gene expression in turtle heart and
497 brain (Stecyk et al., 2012), the density of ion channels in turtle heart (Stecyk et al., 2007) and the gene
498 expression of heat shock proteins in crucian carp heart and brain (Stensløkken et al., 2010). The finding is also
499 in-line with the extensive changes in cardiac gene expression in winter-acclimatized crucian carp that serve to
500 precondition the heart for winter anoxia (Tikkanen et al., 2017). Thus, our data lends further support to the
501 notion that cold acclimation prepares the turtle for a prolonged exposure to anoxia. For instance, the 29%
502 decrease in gene expression of the transcription factor CREB1 (*Creb1*) with cold acclimation could lead to a
503 general reduction of gene transcription in the turtle brain, which is consistent with the general metabolic
504 depression previously described in *C. picta* at low temperature (Herbert and Jackson, 1985). Moreover, 56% of
505 the excitatory neurotransmission genes investigated were down-regulated with cold acclimation, whereas only
506 26% of the inhibitory neurotransmission genes investigated were down-regulated with cold acclimation. The
507 relatively stronger selective downregulation of excitatory neurotransmission may participate to further enhance
508 metabolic depression.

509 Specifically, the gene expression of five of the six NMDAR subunits assessed in the present study
510 (*Grin1*, *Grin2a*, *Grin2b*, *Grin2d* and *Grin3a*, encoding for GluN1, GluN2A, GluN2B, GluN2D and GluN3A,
511 respectively) was reduced with cold acclimation (Fig. 4). NMDARs are glutamate receptors that present a
512 slower response to glutamate than AMPARs (VanDongen, 2008). The receptors are heterotetramers composed
513 of two obligatory GluN1 subunits, the essential component of all functional NMDA receptor complexes, and
514 two of the four GluN2 (GluN2A-D) or two GluN3 (A and B) subunits. In *T. scripta*, the gene expression of
515 GluN1 (*Grin1*) was by far the most abundant compared to the gene expression of all GluN2 and GluN3A
516 subunits, regardless of acclimation temperature or oxygenation state, accounting for approximately 80% of the
517 total GluN gene-family mRNA abundance (Table 4). Therefore, the 36% decreased expression of *Grin1* with
518 cold acclimation supports the 60% decrease in NMDAR abundance and the general downregulation of NMDAR
519 activity previously described in cerebrocortex of anoxic (3-21 days at 3°C) *C. picta* (Bickler et al., 2000).
520 However, as documented here, the decrease in NMDAR gene expression is mainly driven by a decrease in
521 temperature, rather than anoxia *per se*. Gene expression of GluN2A (*Grin2a*) and GluN2B (*Grin2b*), which
522 were the most expressed subunits of the GluN2 gene-family (Table 4), as well as gene expression of GluN2D
523 (*Grin2d*) was also drastically decreased with cold acclimation (Fig. 4). Each GluN2 subunit has a different
524 intracellular C-terminal domain that can interact with different sets of signalling molecules, thereby providing
525 different electrophysiological properties to the NMDA receptor (Loftis and Janowsky, 2003). For instance,
526 NMDARs composed of GluN1/GluN2A and GluN1/GluN2B display a higher sensitivity to voltage-dependent
527 Mg^{2+} block, higher Ca^{2+} permeability, higher single-channel conductance, lower agonist potency and faster
528 deactivation rate than GluN1/GluN2C and GluN1/GluN2D NMDARs (Wyllie et al., 2013). Therefore, the
529 changes in GluN2 subunit gene expression with acclimation to low temperature could indicate a remodelling of
530 the NMDAR activity. Indeed, the relative proportion of *Grin2d* was increased at 5°C compared to 21°C.
531 Although, the change may not play a major role as GluN2D subunit mRNA represented only just above 3% of
532 the total GluN2 gene-family mRNA abundance. Interestingly, the gene expression of GluN3A (*Grin3a*), which
533 is known to exert a dominant-negative effect on NMDAR properties, resulting in an insensitivity to Mg^{2+} and

reduced Ca^{2+} influx compared to the strict GluN1-GluN2 complex (Kehoe et al., 2013; Tong et al., 2008), was also decreased with acclimation temperature. However, the overall decreased gene expression of the GluN1 and GluN2 subunits with cold acclimation suggests a general reduction in NMDAR activation.

In the mammalian brain, reduced NMDAR activity promotes the removal of AMPARs, provoking long-term depression (LTD; Malenka and Bear, 2004). In agreement, AMPAR gene expression was concurrently reduced in turtle telencephalon by acclimation to low temperature. Gene expression of three of the four AMPAR subunits, GluA2 (*Gria2*), GluA3 (*Gria3*) and GluA4 (*Gria4*), showed a significant decrease with cold acclimation (Fig. 4), which resulted in an overall decreased relative gene expression of GluA2 and GluA4 (Table 4). AMPARs are ligand-gated transmembrane glutamate receptors conducting fast excitatory neurotransmission in the synapse. The receptor is a tetramer (a dimer of dimers) composed of 4 subunits (GluA1-4) providing different properties to the channel (Palmer et al., 2005). The presence of GluA2 in the receptor determines many of the major biophysical properties of the receptor, including receptor kinetics and single-channel conductance or Ca^{2+} permeability (Isaac et al., 2007). For example, AMPARs containing the subunit GluA2 are impermeable to Ca^{2+}, whereas those lacking it are Ca^{2+} permeable (Burnashev et al., 1992; Jonas et al., 1994). Thus, the lower expression of *Gria2*, *Gria3* and *Gria4* at low temperature suggests an overall decrease in the abundance of AMPARs in the 5°C turtle brain, and therefore an overall decrease of fast excitatory neurotransmission. Like in mammals (Greger et al., 2007) and the crucian carp (Ellefsen et al., 2008a), GluA2 displayed the highest gene expression of the AMPAR subunits in *T. scripta*, accounting for 38% and 40% of the AMPAR gene family mRNA abundance at 5°C and 21°C, respectively (Table 4). However, unlike in mammals, where GluA1 is the second most abundant AMPAR subunit (Isaac et al., 2007), *Gria3* was the second most abundant AMPAR subunit mRNA in *T. scripta*. *Gria3* expression accounted for 37% and 35% of the total gene family mRNA abundance at 5°C and 21°C, respectively (Table 4). Therefore, while the most abundant receptor subunit composition seems to be GluA1/GluA2 in mammals (Isaac et al., 2007; Reimers et al., 2011), GluA2/GluA3 may be the most abundant in *T. scripta*. In the crucian carp, gene expression data suggest that GluA1 and GluA3 subunits are present in similar abundances (Ellefsen et al., 2008a). Despite a low

559 level of relative expression, the significant decrease in *Gria4* expression with cold acclimation might be related
560 to a reduction of cognitive functions (Sagata et al., 2010).

561 Compared to the changes in gene expression of receptors, transporters, enzymes and regulatory proteins
562 involved in excitatory neurotransmission, relatively fewer changes in the gene expression of receptors,
563 transporters, enzymes and regulatory proteins involved in inhibitory neurotransmission occurred with cold
564 acclimation. $GABA_A$ receptors ($GABA_AR$) are ligand-gated (ionotropic) receptors composed of 5 subunits that
565 upon activation by binding GABA, allows Cl^- through its pore. In mammals, $GABA_AR$ activation results in the
566 fast hyperpolarization of the neuron (Sigel and Steinmann, 2012). By comparison, in *C. picta* cortical neurons,
567 GABA suppresses spontaneous electrical activity via an increase in $GABA_A$ receptor-mediated postsynaptic
568 activity and Cl^- conductance, which dampens excitatory potentials via shunting inhibition (Pamenter et al.,
569 2011). $GABA_B$ receptors ($GABA_BR$) are G protein coupled (metabotropic) transmembrane heterodimers
570 ($GABA_{B1}$ and $GABA_{B2}$) for GABA that mediate a slower response (Mott, 2015). In *C. picta*, GABA decreases
571 excitatory postsynaptic activity via $GABA_BR$-mediated inhibition of presynaptic glutamate release (Pamenter et
572 al., 2011). Among the $GABA_A$ and $GABA_B$ subunits, the gene expression of only three $GABA_A$ subunits was
573 altered with cold acclimation. Specifically, *Graba3* (encodes $GABA_A$ α3), *Graba5* (encodes $GABA_A$ α5) and
574 *Graba6* (encodes $GABA_A$ α6) showed a significantly decreased expression at 5°C compared to at 21°C in
575 normoxia. Notably, the relative gene expression of $GABA_A$ α3, $GABA_A$ α5 and $GABA_A$ α6 was the least among
576 the $GABA_A$ subunit gene family (Table 4). Nevertheless, even at a low level, the change in GABA receptor
577 subunit gene expression could be important, as any switch in GABA receptor subunit usage can have a massive
578 effect on function (Hevers and Luddens, 1998). As in mammals (Whiting, 2003), and contrary to the crucian
579 carp (Ellefsen et al., 2009), $GABA_A$ α1 displayed the greatest relative gene expression among the $GABA_A$ α
580 subunits. Also like in mammals, but contrary to the crucian carp (Ellefsen et al., 2009), the relative gene
581 expression of $GABA_A$ γ2 was greater than $GABA_A$ δ, suggesting that synaptic $GABA_AR$s play a more
582 prominent role than extrasynaptic ones (Ellefsen et al., 2009). It has been proposed that the subunit composition
583 of $GABA_AR$s in the crucian carp brain could represent a constitutive preconditioning i.e., a selective advantage

584 during anoxic insults (Ellefsen et al., 2009). In this context, the more similar $GABA_AR$ subunit gene expression
585 of *T. scripta* to mammals than crucian carp could be related to the divergent anoxia survival strategies of the
586 fish and the turtle. The crucian carp remains active in anoxia while *T. scripta* is nearly comatose (Nilsson and
587 Lutz, 2004). As in mammals, gene expression of GAT1 (*Slc6a1*) and GAT3 (*Slc6a11*) were greatest of all the
588 GABA transporters measured (Table 4), and while the gene expression of GAT1 was maintained with cold
589 acclimation, the gene expression of GAT2 (*Slc6a13*) and GAT3 showed a respective decrease and increase at
590 5°C compared to 21°C. In the mammalian brain, GAT1 is prominent in the synapse while GAT2 and 3 are more
591 abundant outside of the synapse (Conti et al., 2004). The decreased gene expression of GAT1 and GAT2 with
592 cold acclimation in *T. scripta* might limit GABA removal from the extracellular space to facilitate GABAergic
593 inhibition at the synapse, thereby suppressing neural activity and ATP use.
594 Normal GABA neurotransmission is also dependent on the precise regulation of intracellular chloride,
595 which is determined by the coordinated activities of two cation/chloride cotransporters: the chloride ion
596 transporter (KCC2) and the Na-K-Cl cotransporter 1 (NKCC1). KCC2 establishes the chloride ion gradient
597 necessary for postsynaptic inhibition, driving Cl^- out of the neuron, and strongly influences the efficacy and
598 polarity of the $GABA_AR$ mediated synaptic transmission (Chamma et al., 2012). NKCC1 symporters
599 cotransport sodium (Na^+), potassium (K^+), and chloride (Cl^-) ions inside the cell to help maintain
600 electroneutrality. With cold acclimation, the gene expression of KCC2 (*Slc12a5*) remained stable whereas the
601 gene expression of NKCC1 (*Slc12a2*) showed a significant decrease. An explanation for why gene expression
602 of KCC2 was not downregulated with cold temperature (or anoxia) is a possible role of KCC2 in the protection
603 of neurons against excitotoxicity. KCC2 has been shown to be expressed at the vicinity of not only inhibitory
604 synapses but also excitatory ones (Gulyás et al., 2001). KCC2 could be involved in the regulation of ion flow
605 through the membrane to prevent osmotic swelling during excitatory synaptic stimulation.
606
607 **Concluding Remarks**

In conclusion, the present study points to key responses at the transcriptional level that are congruous with synaptic arrest, and thereby neuronal tolerance of anoxia and reoxygenation in the turtle brain. The observed changes in gene expression of key receptors, transporters, enzymes and regulatory proteins involved in excitatory and inhibitory transmission in the anoxic turtle brain could contribute to the decline in glutamatergic activity and the increase in GABAergic activity observed at cellular and whole organism levels. In addition, the substantial transcriptional response observed in turtles acclimated from 21°C to 5°C in normoxia, namely the pronounced downregulation of excitatory neurotransmission gene, emphasizes the importance of cold acclimation in preparing the turtle brain for prolonged anoxia survival in winter. Future research should focus on identifying how neuronal gene expression in the anoxic turtle brain is regulated by post-transcriptional, translational and post-translational modifications.

Acknowledgments

This research was financed by the Research Council of Norway (to G.E.N. - FRIMEDBIO 231260). J.A.W.S. was supported by a NSERC post-doctoral fellowship. We thank Tove K. Larsen and Cathrine E. Fagernes for technical assistance.

Author contributions

Conceptualization: G.N., S.M., H.P.; Investigation: C.C., J.S., S.E., G.S.; Formal analysis: C.C.; Writing - original draft: C.C., J.S.; Writing - review & editing: C.C., J.S., G.N., S.E., S.M., H.P; Funding acquisition: G.N. The authors declare no competing interests.

References

Alkallas, R., Fish, L., Goodarzi, H., Najafabadi, H.S., 2017. Inference of RNA decay rate from transcriptional profiling highlights the regulatory programs of Alzheimer's disease. Nat. Commun. 8, 909.

Bahrami, S., Drabløs, F., 2016. Gene regulation in the immediate-early response process. Adv. Biol. Regul. 62, 37-49.

Bansal, S., Biggar, K.K., Krivoruchko, A., Storey, K.B., 2016. Response of the JAK-STAT signaling pathway to oxygen deprivation in the red eared slider turtle, *Trachemys scripta elegans*. Gene 593, 34-40.

Bickler, P.E., 1998. Reduction of NMDA receptor activity in cerebrocortex of turtles (*Chrysemys picta*) during 6 wk of anoxia. Am. J. Physiol. 275, R86-91.

Bickler, P.E., Donohoe, P.H., Bucks, L.T., 2000. Hypoxia-induced silencing of NMDA receptors in turtle neurons. J. Neurosci. 20, 3522-3528.

Biggar, K.K., Storey, K.B., 2011. The emerging roles of microRNAs in the molecular responses of metabolic rate depression. J. Mol. Cell Biol. 3, 167-175.

Biggar, K.K., Storey, K.B., 2015. Insight into post-transcriptional gene regulation: stress-responsive microRNAs and their role in the environmental stress survival of tolerant animals. J. Exp. Biol. 218, 1281-1289.

Buck, L.T., Bickler, P.E., 1998. Adenosine and anoxia reduce N-methyl-D-aspartate receptor open probability in turtle cerebrocortex. J. Exp. Biol. 201, 289-297.

Buck, L.T., Pamenter, M.E., 2018. The hypoxia-tolerant vertebrate brain: arresting synaptic activity. Comp. Biochem. Physiol. B-Biochem. Mol. Biol. 224, 61-70.

Burnashev, N., Monyer, H., Seeburg, P.H., Sakmann, B., 1992. Divalent ion permeability of AMPA receptor channels is dominated by the edited form of a single subunit. Neuron 8, 189-198.

Chamma, I., Chevy, Q., Poncer, J.C., Lévi, S., 2012. Role of the neuronal K-Cl co-transporter KCC2 in inhibitory and excitatory neurotransmission. Front. Cell. Neurosci. 6, 5.

Chowdhury, S., Shepherd, J.D., Okuno, H., Lyford, G., Petralia, R.S., Plath, N., Kuhl, D., Huganir, R.L., Worley, P.F., 2006. Arc/Arg3.1 interacts with the endocytic machinery to regulate AMPA receptor trafficking. Neuron 52, 445-459.

Cikos, S., Bukovska, A., Koppel, J., 2007. Relative quantification of mRNA: comparison of methods currently used for real-time PCR data analysis. BMC Mol. Biol. 8, 113.

Conti, F., Minelli, A., Melone, M., 2004. GABA transporters in the mammalian cerebral cortex: localization, development and pathological implications. Brain Res. Rev. 45, 196-212.

Del Toro, R., Levitsky, K.L., Lopez-Barneo, J., Chiara, M.D., 2003. Induction of T-type calcium channel gene expression by chronic hypoxia. J. Biol. Chem. 278, 22316-22324.

Ellefsen, S., Sandvik, G.K., Larsen, H.K., Stensløkken, K.-O., Hov, D.A.S., Kristensen, T.A., Nilsson, G.E., 2008a. Expression of genes involved in excitatory neurotransmission in anoxic crucian carp (*Carassius carassius*) brain. Physiol. Genomics 35, 5-17.

Ellefsen, S., Stensløkken, K.-O., Fagernes, C., Kristensen, T.A., Nilsson, G.E., 2009. Expression of genes involved in GABAergic neurotransmission in anoxic crucian carp brain (*Carassius carassius*). Physiol. Genomics 36, 61-68.

Ellefsen, S., Stensløkken, K.-O., Sandvik, G.K., Kristensen, T.A., Nilsson, G.E., 2008b. Improved normalization of real-time reverse transcriptase polymerase chain reaction data using an external RNA control. Anal. Biochem. 376, 83-93.

Ellefsen, S., Stenslokken, K.O., 2010. Gene-family profiling: a normalization-free real-time RT-PCR approach with increased physiological resolution. Physiol. Genomics 42, 1-4.

Fraser, K.P.P., Houlihan, D.F., Lutz, P.L., Leone-Kabler, S., Manuel, L., Brechin, J.G., 2001. Complete suppression of protein synthesis during anoxia with no post-anoxia protein synthesis debt in the red-eared slider turtle *Trachemys scripta elegans*. J. Exp. Biol. 204, 4353-4360.

Furness, D.N., Dehnes, Y., Akhtar, A.Q., Rossi, D.J., Hamann, M., Grutle, N.J., Gundersen, V., Holmseth, S., Lehre, K.P., Ullensvang, K., Wojewodzic, M., Zhou, Y., Attwell, D., Danbolt, N.C., 2008. A quantitative assessment of glutamate uptake into hippocampal synaptic terminals and astrocytes: new insights into a neuronal role for excitatory amino acid transporter 2 (EAAT2). Neuroscience 157, 80-94.

Giorgi, C., Yeo, G.W., Stone, M.E., Katz, D.B., Burge, C., Turrigiano, G., Moore, M.J., 2007. The EJC Factor eIF4AIII Modulates Synaptic Strength and Neuronal Protein Expression. Cell 130, 179-191.

Greenway, S.C., Storey, K.B., 2000. Mitogen-activated protein kinases and anoxia tolerance in turtles. J. Exp. Zool. 287, 477-484.

Greger, I.H., Ziff, E.B., Penn, A.C., 2007. Molecular determinants of AMPA receptor subunit assembly. Trends Neurosci. 30, 407-416.

Gulyás, A.I., Sík, A., Payne, J.A., Kaila, K., Freund, T.F., 2001. The KCl cotransporter, KCC2, is highly expressed in the vicinity of excitatory synapses in the rat hippocampus. Eur. J. Neurosci. 13, 2205-2217.

Hammer, Ø., Harper, D.A.T., Ryan, P.D., 2001. PAST: Paleontological statistics software package for education and data analysis. Palaeontologia Electronica 4, 9pp.

Hellemans, J., Vandesompele, J., 2011. qPCR data analysis - unlocking the secret to successful results, in: S. Kennedy, N. Oswald (Eds.), PCR troubleshooting and optimization: the essential guide. Caister Academic Press.

Herbert, C.V., Jackson, D.C., 1985. Temperature effects on the responses to prolonged submergence in the turtle *Chrysemys picta bellii*. II. Metabolic rate, blood acid-base and ionic changes, and cardiovascular function in aerated and anoxic water. Physiol. Zool. 58, 670-681.

Hevers, W., Luddens, H., 1998. The diversity of GABAA receptors. Pharmacological and electrophysiological properties of GABAA channel subtypes. Mol. Neurobiol. 18, 35-86.

Hicks, J.M., Farrell, A.P., 2000. The cardiovascular responses of the red-eared slider (*Trachemys scripta*) acclimated to either 22 or 5 degrees C. I. Effects of anoxic exposure on in vivo cardiac performance. J. Exp. Biol. 203, 3765-3774.

Hochachka, P.W., 1986. Defense strategies against hypoxia and hypothermia. Science 231, 234-241.

Hogg, D.W., Hawrysh, P.J., Buck, L.T., 2014. Environmental remodelling of GABAergic and glutamatergic neurotransmission: Rise of the anoxia-tolerant turtle brain. J. Therm. Biol. 44, 85-92.

Holmseth, S., Dehnes, Y., Huang, Y.H., Follin-Arbelet, V.V., Grutle, N.J., Mylonakou, M.N., Plachez, C., Zhou, Y., Furness, D.N., Bergles, D.E., Lehre, K.P., Danbolt, N.C., 2012. The density of EAAC1 (EAAT3) glutamate transporters expressed by neurons in the mammalian CNS. J. Neurosci. 32, 6000-6013.

Hylland, P., Milton, S., Pek, M., Nilsson, G.E., L. Lutz, P., 1997. Brain Na^+/K^+-ATPase activity in two anoxia tolerant vertebrates: crucian carp and freshwater turtle. Neurosci. Lett. 235, 89-92.

Isaac, J.T.R., Ashby, M.C., McBain, C.J., 2007. The role of the GluR2 subunit in AMPA receptor function and synaptic plasticity. Neuron 54, 859-871.

Jackson, D.C., 1968. Metabolic depression and oxygen depletion in the diving turtle. J. Appl. Physiol 24, 503-509.

Jackson, D.C., 2000a. How a turtle's shell helps it survive prolonged anoxic acidosis. Physiol. 15, 181-185.

Jackson, D.C., 2000b. Living without oxygen: lessons from the freshwater turtle. Comp Biochem Physiol A Mol Integr Physiol 125, 299-315.

Jackson, D.C., Ultsch, G.R., 2010. Physiology of hibernation under the ice by turtles and frogs. J. Exp. Zool. Part A 313A, 311-327.

Jonas, P., Racca, C., Sakmann, B., Seeburg, P.H., Monyer, H., 1994. Differences in Ca^{2+} permeability of AMPA-type glutamate receptor channels in neocortical neurons caused by differential GluR-B subunit expression. Neuron 12, 1281-1289.

Keenan, S.W., Hill, C.A., Kandoth, C., Buck, L.T., Warren, D.E., 2015. Transcriptomic responses of the heart and brain to anoxia in the western painted turtle. PLoS ONE 10, e0131669.

Kehoe, L.A., Bernardinelli, Y., Muller, D., 2013. GluN3A: an NMDA receptor subunit with exquisite properties and functions. Neural Plast. 2013, 12.

Kesaraju, S., Schmidt-Kastner, R., Prentice, H.M., Milton, S.L., 2009. Modulation of stress proteins and apoptotic regulators in the anoxia tolerant turtle brain. J. Neurochem. 109, 1413-1426.

Korb, E., Finkbeiner, S., 2011. Arc in synaptic plasticity: from gene to behavior. Trends Neurosci. 34, 591-598.

Krivoruchko, A., Storey, K.B., 2010a. Molecular mechanisms of turtle anoxia tolerance: A role for NF-κB. Gene 450, 63-69.

Krivoruchko, A., Storey, K.B., 2010b. Regulation of the heat shock response under anoxia in the turtle, *Trachemys scripta elegans*. J. Comp. Physiol. B-Biochem. Syst. Environ. Physiol. 180, 403-414.

Krivoruchko, A., Storey, K.B., 2013. Anoxia-responsive regulation of the FoxO transcription factors in freshwater turtles, *Trachemys scripta elegans*. Biochim. Biophys. Acta 1830, 4990-4998.

Loftis, J.M., Janowsky, A., 2003. The N-methyl-d-aspartate receptor subunit NR2B: localization, functional properties, regulation, and clinical implications. Pharmacol. Ther. 97, 55-85.

Lutz, P.L., Leone-Kabler, S.L., 1995. Upregulation of the GABAA/benzodiazepine receptor during anoxia in the freshwater turtle brain. Am. J. Physiol.-Regul. Integr. Comp. Physiol. R268, 1332-1335.

Lutz, P.L., McMahon, P., Rosenthal, M., Sick, T.J., 1984. Relationships between aerobic and anaerobic energy production in turtle brain in situ. Am. J. Physiol. 247, R740-744.

Lutz, P.L., Nilsson, G.E., 1997. Contrasting strategies for anoxic brain survival - glycolysis up or down. J. Exp. Biol. 200, 411-419.

Luu-The, V., Paquet, N., Calvo, E., Cumps, J., 2005. Improved real-time RT-PCR method for high-throughput measurements using second derivative calculation and double correction. BioTechniques 38, 287-293.

Malenka, R.C., Bear, M.F., 2004. LTP and LTD: an embarrassment of riches. Neuron 44, 5-21.

Mott, D., 2015. Chapter 11 - The metabotropic GABAB receptors, in: C. Hammond (Ed.), Cellular and Molecular Neurophysiology (Fourth Edition). Academic Press, Boston, 245-267.

Nilsson, G.E., 2001. Surviving anoxia with the brain turned on. News Physiol. Sci. 16, 217-221.

Nilsson, G.E., Lutz, P.L., 1991. Release of inhibitory neurotransmitters in response to anoxia in turtle brain. Am. J. Physiol.-Regul. Integr. Comp. Physiol. R261, 32-37.

Nilsson, G.E., Lutz, P.L., 2004. Anoxia tolerant brains. J. Cereb. Blood Flow Metab. 24, 475-486.

Palmer, C.L., Cotton, L., Henley, J.M., 2005. The molecular pharmacology and cell biology of α-amino-3-hydroxy-5-methyl-4-isoxazolepropionic acid receptors. Pharmacological reviews 57, 253-277.

Pamenter, M.E., Hogg, D.W., Ormond, J., Shin, D.S., Woodin, M.A., Buck, L.T., 2011. Endogenous GABAA and GABAB receptor-mediated electrical suppression is critical to neuronal anoxia tolerance. Proc. Natl. Acad. Sci. U. S. A.

Pamenter, M.E., Shin, D.S., Cooray, M., Buck, L.T., 2008a. Mitochondrial ATP-sensitive K+ channels regulate NMDAR activity in the cortex of the anoxic western painted turtle. J. Physiol. 586, 1043-1058.

Pamenter, M.E., Shin, D.S.H., Buck, L.T., 2008b. AMPA receptors undergo channel arrest in the anoxic turtle cortex. Am. J. Physiol.-Regul. Integr. Comp. Physiol. 294, R606-R613.

Prentice, H.M., Milton, S.L., Scheurle, D., Lutz, P.L., 2003. Gene transcription of brain voltage-gated potassium channels is reversibly regulated by oxygen supply. Am. J. Physiol.-Regul. Integr. Comp. Physiol. 285, R1317–R1321.

R Development Core Team, 2009. R: a language and environment for statistical computing. R Foundation for Statistical Computing, Vienna, Austria.

Reimers, J.M., Milovanovic, M., Wolf, M.E., 2011. Quantitative analysis of AMPA receptor subunit composition in addiction-related brain regions. Brain Res. 1367, 223-233.

Rial Verde, E.M., Lee-Osbourne, J., Worley, P.F., Malinow, R., Cline, H.T., 2006. Increased expression of the immediate-early gene arc/arg3.1 reduces AMPA receptor-mediated synaptic transmission. Neuron 52, 461-474.

Roberts, R.C., Roche, J.K., McCullumsmith, R.E., 2014. Localization of excitatory amino acid transporters EAAT1 and EAAT2 in human postmortem cortex: a light and electron microscopic study. Neuroscience 277, 522-540.

Rozen, S., Skaletsky, H., 2000. Primer3 on the WWW for general users and for biologist programmers, Bioinformatics Methods and Protocols, 365-386.

Ruijter, J.M., Ramakers, C., Hoogaars, W.M.H., Karlen, Y., Bakker, O., van den Hoff, M.J.B., Moorman, A.F.M., 2009. Amplification efficiency: linking baseline and bias in the analysis of quantitative PCR data. Nucleic Acids Res. 37, e45.

Sagata, N., Iwaki, A., Aramaki, T., Takao, K., Kura, S., Tsuzuki, T., Kawakami, R., Ito, I., Kitamura, T., Sugiyama, H., Miyakawa, T., Fukumaki, Y., 2010. Comprehensive behavioural study of GluR4 knockout mice: implication in cognitive function. Genes Brain Behav. 9, 899-909.

Saxena, N.C., Macdonald, R.L., 1994. Assembly of GABAA receptor subunits: role of the delta subunit. J. Neurosci. 14, 7077-7086.

Selcher, J.C., Xu, W., Hanson, J.E., Malenka, R.C., Madison, D.V., 2012. Glutamate receptor subunit GluA1 is necessary for long-term potentiation and synapse unsilencing, but not long-term depression in mouse hippocampus. Brain Res. 1435, 8-14.

Sigel, E., Steinmann, M.E., 2012. Structure, function, and modulation of GABAA receptors. J. Biol. Chem. 287, 40224-40231.

Smith, T.A., 2001. Type A gamma-aminobutyric acid (GABAA) receptor subunits and benzodiazepine binding: significance to clinical syndromes and their treatment. Br. J. Biomed. Sci. 58, 111-121.

Stecyk, J.A.W., 2017. Cardiovascular responses to limiting oxygen levels, in: A.K. Gamperl, T.E. Gillis, A.P. Farrell, C.J. Brauner (Eds.), Fish Physiology. Academic Press, 299-371.

Stecyk, J.A.W., Couturier, C.S., Fagernes, C.E., Ellefsen, S., Nilsson, G.E., 2012. Quantification of heat shock protein mRNA expression in warm and cold anoxic turtles (*Trachemys scripta*) using an external RNA control for normalization. Comp. Biochem. Physiol. D-Genomics Proteomics 7, 59-72.

Stecyk, J.A.W., Farrell, A.P., Vornanen, M., 2017. Na+/K+-ATPase activity in the anoxic turtle (*Trachemys scripta*) brain at different acclimation temperature. Comp. Biochem. Physiol. A-Mol. Integr. Physiol. 206, 11-16.

Stecyk, J.A.W., Galli, G.L., Shiels, H.A., Farrell, A.P., 2008. Cardiac survival in anoxia-tolerant vertebrates: An electrophysiological perspective. Comp Biochem Physiol C-Toxicol. Pharmacol. 148, 339-354.

875 Stecyk, J.A.W., Overgaard, J., Farrell, A.P., Wang, T., 2004. alpha-Adrenergic regulation of systemic
876 peripheral resistance and blood flow distribution in the turtle Trachemys scripta during anoxic submergence at 5
877 degrees C and 21 degrees C. J. Exp. Biol. 207, 269-283.
878
879 Stecyk, J.A.W., Paajanen, V., Farrell, A.P., Vornanen, M., 2007. Effect of temperature and prolonged anoxia
880 exposure on electrophysiological properties of the turtle (*Trachemys scripta*) heart. Am. J. Physiol.-Regul.
881 Integr. Comp. Physiol. 293, R421-R437.
882
883 Stensløkken, K.-O., Ellefsen, S., Larsen, H.K., Vaage, J., Nilsson, G.E., 2010. Expression of heat shock proteins
884 in anoxic crucian carp (*Carassius carassius*): support for cold as a preparatory cue for anoxia. Am. J. Physiol.-
885 Regul. Integr. Comp. Physiol. 298, R1499-R1508.
886
887 Suchak, S.K., Baloyianni, N.V., Perkinton, M.S., Williams, R.J., Meldrum, B.S., Rattray, M., 2003. The 'glial'
888 glutamate transporter, EAAT2 (Glt-1) accounts for high affinity glutamate uptake into adult rodent nerve
889 endings. J. Neurochem. 84, 522-532.
890
891 Tanaka, K., Watase, K., Manabe, T., Yamada, K., Watanabe, M., Takahashi, K., Iwama, H., Nishikawa, T.,
892 Ichihara, N., Kikuchi, T., Okuyama, S., Kawashima, N., Hori, S., Takimoto, M., Wada, K., 1997. Epilepsy and
893 exacerbation of brain injury in mice lacking the glutamate transporter GLT-1. Science 276, 1699-1702.
894
895 Thompson, J.D., Gibson, T.J., Plewniak, F., Jeanmougin, F., Higgins, D.G., 1997. The CLUSTAL_X Windows
896 Interface: Flexible Strategies for Multiple Sequence Alignment Aided by Quality Analysis Tools. Nucleic Acids
897 Res. 25, 4876-4882.
898
899 Thompson, J.W., Prentice, H.M., Lutz, P.L., 2007. Regulation of extracellular glutamate levels in the long-term
900 anoxic turtle striatum: coordinated activity of glutamate transporters, adenosine, K-ATP^{+} channels and GABA.
901 J. Biomed. Sci. 14, 809-817.
902
903 Tikkanen, E., Haverinen, J., Egginton, S., Hassinen, M., Vornanen, M., 2017. Effects of prolonged anoxia on
904 electrical activity of the heart in crucian carp (*Carassius carassius*). J. Exp. Biol. 220, 445-454.
905
906 Tong, G., Takahashi, H., Tu, S., Shin, Y., Talantova, M., Zago, W., Xia, P., Nie, Z., Goetz, T., Zhang, D.,
907 Lipton, S.A., Nakanishi, N., 2008. Modulation of NMDA receptor properties and synaptic transmission by the
908 NR3A subunit in mouse hippocampal and cerebrocortical neurons. J. Neurophysiol. 99, 122-132.
909
910 Ultsch, G.R., 1985. The viability of nearctic freshwater turtles submerged in anoxia and normoxia at 3 and
911 10°C. Comp. Biochem. Physiol. A-Physiol. 81, 607-611.
912
913 Ultsch, G.R., 2006. The ecology of overwintering among turtles: where turtles overwinter and its consequences.
914 Biol. Rev. Camb. Philos. Soc. 81, 339-367.
915
916 VanDongen, A.M., 2008. Biology of the NMDA Receptor. CRC Press.
917 https://www.ncbi.nlm.nih.gov/books/NBK5283/
918
919 Vornanen, M., Stecyk, J.A.W., Nilsson, G.E., 2009. The anoxia-tolerant crucian carp (*Carassius carassius*, L.),
920 in: J.G. Richards, A.P. Farrell, C.J. Brauner (Eds.), Hypoxia. Academic Press, 397-441.
921
922 Wang, H., Bedford, F.K., Brandon, N.J., Moss, S.J., Olsen, R.W., 1999. $GABA_A$-receptor-associated protein
923 links $GABA_A$ receptors and the cytoskeleton. Nature 397, 69-72.
924

925 Warren, D.E., Jackson, D.C., 2007. Effects of temperature on anoxic submergence: skeletal buffering, lactate
926 distribution, and glycogen utilization in the turtle, Trachemys scripta. Am. J. Physiol.-Regul. Integr. Comp.
927 Physiol. 293, R458-R467.
928
929
930 Warren, D.E., Reese, Scott A., Jackson, Donald C., 2006. Tissue glycogen and extracellular buffering limit the
931 survival of red-eared slider turtles during anoxic submergence at 3°C. Physiol. Biochem. Zool. 79, 736-744.
932
933 Whiting, P.J., 2003. GABA-A receptor subtypes in the brain: a paradigm for CNS drug discovery? Drug
934 Discov. Today 8, 445-450.
935
936 Wijenayake, S., Hawkins, L.J., Storey, K.B., 2018. Dynamic regulation of six histone H3 lysine (K)
937 methyltransferases in response to prolonged anoxia exposure in a freshwater turtle. Gene 649, 50-57.
938
939 Wilson, C.M., Stecyk, J.A.W., Couturier, C.S., Nilsson, G.E., Farrell, A.P., 2013. Phylogeny and effects of
940 anoxia on hyperpolarization-activated cyclic nucleotide-gated channel gene expression in the heart of a
941 primitive chordate, the Pacific hagfish (*Eptatretus stoutii*). J. Exp. Biol. 216, 4462-4472.
942
943 Wyllie, D.J.A., Livesey, M.R., Hardingham, G.E., 2013. Influence of GluN2 subunit identity on NMDA
944 receptor function. Neuropharmacology 74, 4-17.
945
946 Zhang, J., Biggar, K.K., Storey, K.B., 2013. Regulation of p53 by reversible post-transcriptional and post-
947 translational mechanisms in liver and skeletal muscle of an anoxia tolerant turtle, *Trachemys scripta elegans*.
948 Gene 513, 147-155.
949
950 Zivkovic, G., Buck, L.T., 2010. Regulation of AMPA receptor currents by mitochondrial ATP-sensitive K^+
951 channels in anoxic turtle neurons. J. Neurophysiol. 104, 1913-1922.
952

Fig. 1. Statistically significantly altered genes involved in excitatory (in white) and inhibitory (in grey) neurotransmission pathways in telencephalon of 21°C-acclimated *Trachemys scripta* exposed to normoxia (N1), anoxia (A1) and after reoxygenation (A1N1), as detailed in Table 2. The complete dataset for all measured genes under these oxygenation states is provided in Table 3. Data sets are normalized to the external RNA control mw2060 and referenced to the control normoxic turtles. The protein encoded by each gene is provided in parentheses with the gene name. Statistical analysis: One-way ANOVA (*P*- and *F*-values are provided in Table S1) and Tukey HSD *post hoc* test (dissimilar letters above the bars indicate statistically significant differences among exposure groups for each gene). Values are means ±SEM. N=7-8 per exposure group.

Fig.2 Expression profiles (%) per exposure condition for gene-family profiles presenting statistically significant differences between (a) normoxia, anoxia and reoxygenation at 21°C, (b) normoxia, anoxia and reoxygenation at 5°C, and (c) 21°C and 5°C in normoxia. For abbreviations of oxygenation state see Table 2. The complete dataset for all measured genes under these oxygenation states is provided in Table 4. Statistical analysis for panels (a) and (b): one-way ANOVA (*P*- and *F*-values are provided in Table S2) and Tukey HSD *post hoc* test (dissimilar letters associated with a subunit indicate statistically significant differences among exposure groups for that gene). Statistical analysis for panel (c): Student's *t*-test (asterisks associated with a subunit indicate the level of significance for that gene: * $P < 0.05$, ** $P < 0.01$, *** $P < 0.001$; *P*-values and *t*-ratios are provided in Table S2). Values are means ±SEM. N=7-10 per exposure group.

Fig. 3 Statistically significantly altered genes involved in excitatory (in white) and inhibitory (in grey) neurotransmission pathways in telencephalon of 5°C-acclimated *Trachemys scripta* exposed to normoxia (N14), anoxia (A1 and A14) and after reoxygenation (A14N13), as detailed in Table 2. The complete dataset for all measured genes under these oxygenation states is provided in Table 5. Data sets are normalized to the external RNA control mw2060 and referenced to the control normoxic turtles. The protein encoded by each gene is provided in parentheses with the gene name. Statistical analysis: One-way ANOVA (*P*- and *F*-values are provided in Table S3) and Tukey HSD *post hoc* test (dissimilar letters above the bars indicate statistically significant differences among exposure groups for each gene). Values are means ±SEM. N=9-10 per exposure group.

Fig 4. Relative expression of genes involved in (a) excitatory and (b) inhibitory neurotransmission pathways in *Trachemys scripta* telencephalon in normoxia at 5°C compared to normoxia at 21°C. Data sets were normalized to the external RNA control mw2060 and referenced to the 21°C turtles (= 1.00 for each gene). The protein encoded by each gene is provided (corresponding gene names are provided in Table 1). Statistical analysis: Student's *t*-test; level of significance: * $P < 0.05$, ** $P < 0.01$, *** $P < 0.001$ (*P*-values and *t*-ratios are provided in Table S4). Values are means ±SEM. N=8-9 per exposure group.

Fig 5. Principle component analysis (PCA) plots (PC1 versus PC2) of gene expression (39 target genes) in telencephalon of *Trachemys scripta* (a) exposed to normoxia, anoxia or reoxygenation at 21°C, (b) exposed to normoxia, anoxia or reoxygenation at 5°C and (c) acclimated to 21°C or 5°C in normoxia. For abbreviations of oxygenation state see Table 2. Each point represents the gene expression profile of an individual turtle within an exposure condition and the coordinates correspond to the specific value measured for the subject on the corresponding principal component. Corresponding factor maps demonstrate the contribution of the response variables (i.e., the 39 gene targets symbolized by arrows; corresponding protein names are listed) to the principle components. The length of the arrow is directional proportional with the contribution of variance of each gene to the total variability. The color gradient highlights the most important genes in explaining the variation (contribution %) retained by the principle components. The scree plots of eigenvalues (insets) depict the proportion of variance of the first six principle components.

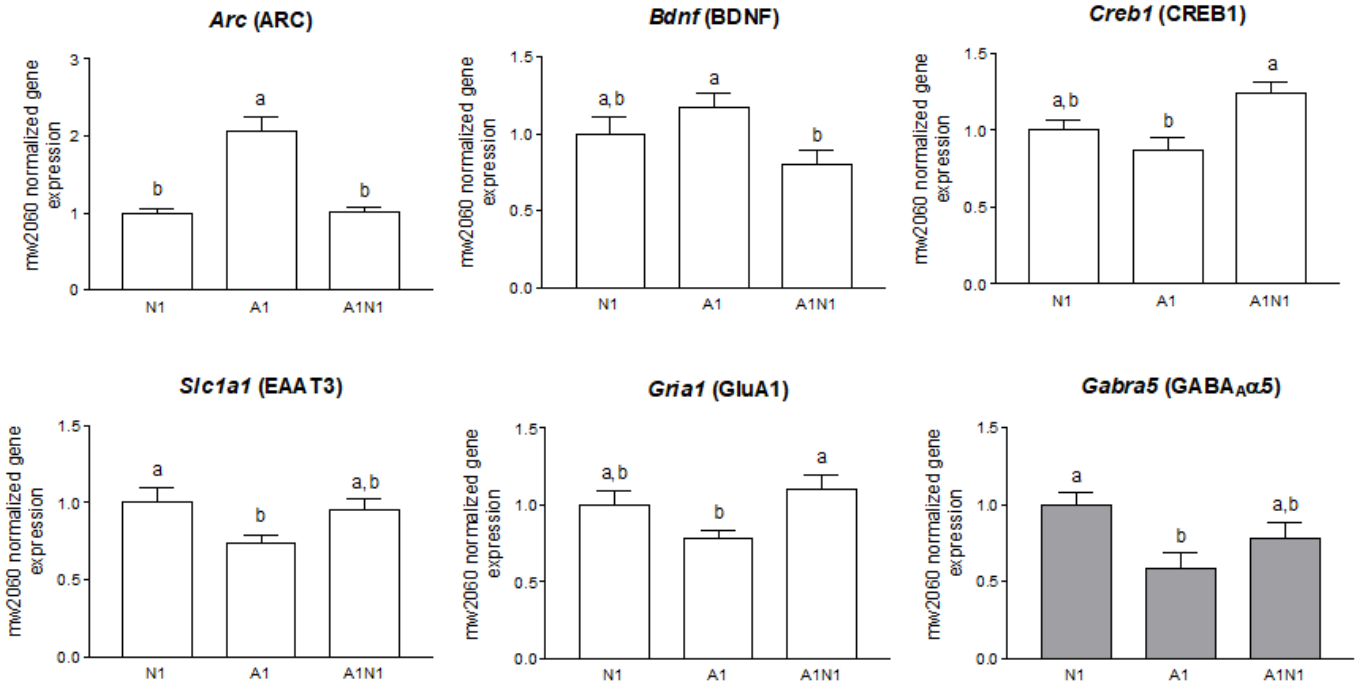
Arc (ARC)
Bdnf (BDNF)
Creb1 (CREB1)
Slc1a1 (EAAT3)
Gria1 (GluA1)
Gabra5 (GABAAα5)
rnw2060 normalized gene expression
N1
A1
A1N1
a
b
a,b

Figure 1.

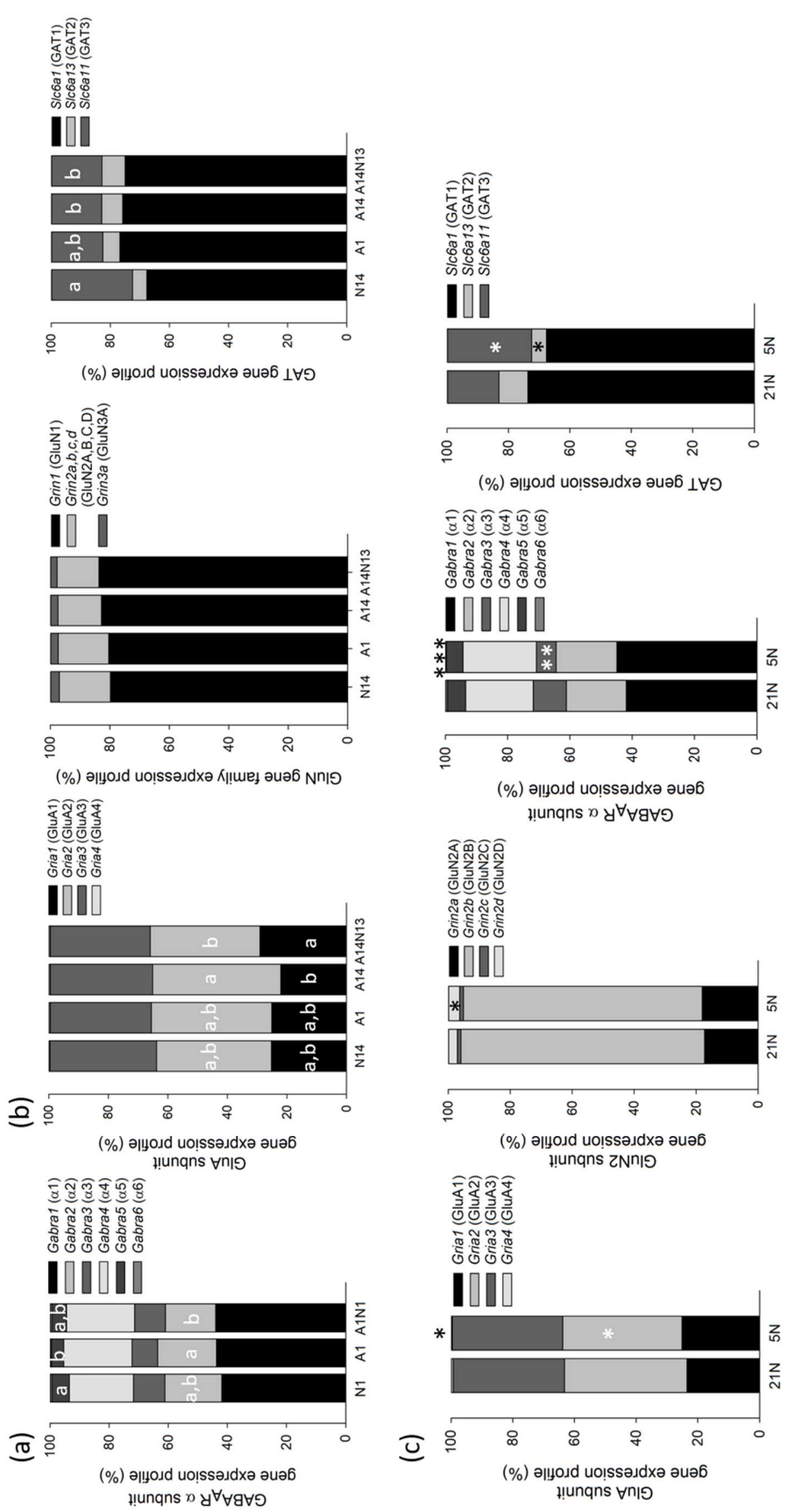
(a)
GABAAR α subunit gene expression profile (%)
Gabra1 (α1)
Gabra2 (α2)
Gabra3 (α3)
Gabra4 (α4)
Gabra5 (α5)
Gabra6 (α6)
N1 A1 A1N1
(b)
GluA subunit gene expression profile (%)
Gria1 (GluA1)
Gria2 (GluA2)
Gria3 (GluA3)
Gria4 (GluA4)
N14 A1 A14 A14N13
GluN gene family expression profile (%)
Grin1 (GluN1)
Grin2a,b,c,d (GluN2A,B,C,D)
Grin3a (GluN3A)
N14 A1 A14 A14N13
GAT gene expression profile (%)
Slc6a1 (GAT1)
Slc6a13 (GAT2)
Slc6a11 (GAT3)
N14 A1 A14 A14N13
(c)
GluA subunit gene expression profile (%)
Gria1 (GluA1)
Gria2 (GluA2)
Gria3 (GluA3)
Gria4 (GluA4)
21N 5N
GluN2 subunit gene expression profile (%)
Grin2a (GluN2A)
Grin2b (GluN2B)
Grin2c (GluN2C)
Grin2d (GluN2D)
21N 5N
GABAAR α subunit gene expression profile (%)
Gabra1 (α1)
Gabra2 (α2)
Gabra3 (α3)
Gabra4 (α4)
Gabra5 (α5)
Gabra6 (α6)
21N 5N
GAT gene expression profile (%)
Slc6a1 (GAT1)
Slc6a13 (GAT2)
Slc6a11 (GAT3)
21N 5N

Figure 2.

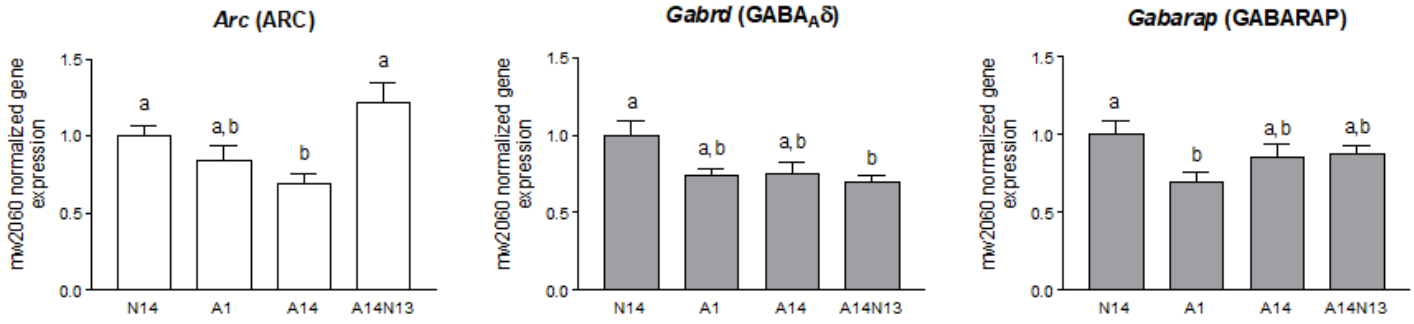
Arc (ARC)
Gabrd (GABA$_A$δ)
Gabarap (GABARAP)
mw2060 normalized gene expression
1.5
1.0
0.5
0.0
a
a,b
b
a
N14
A1
A14
A14N13

Figure 3.

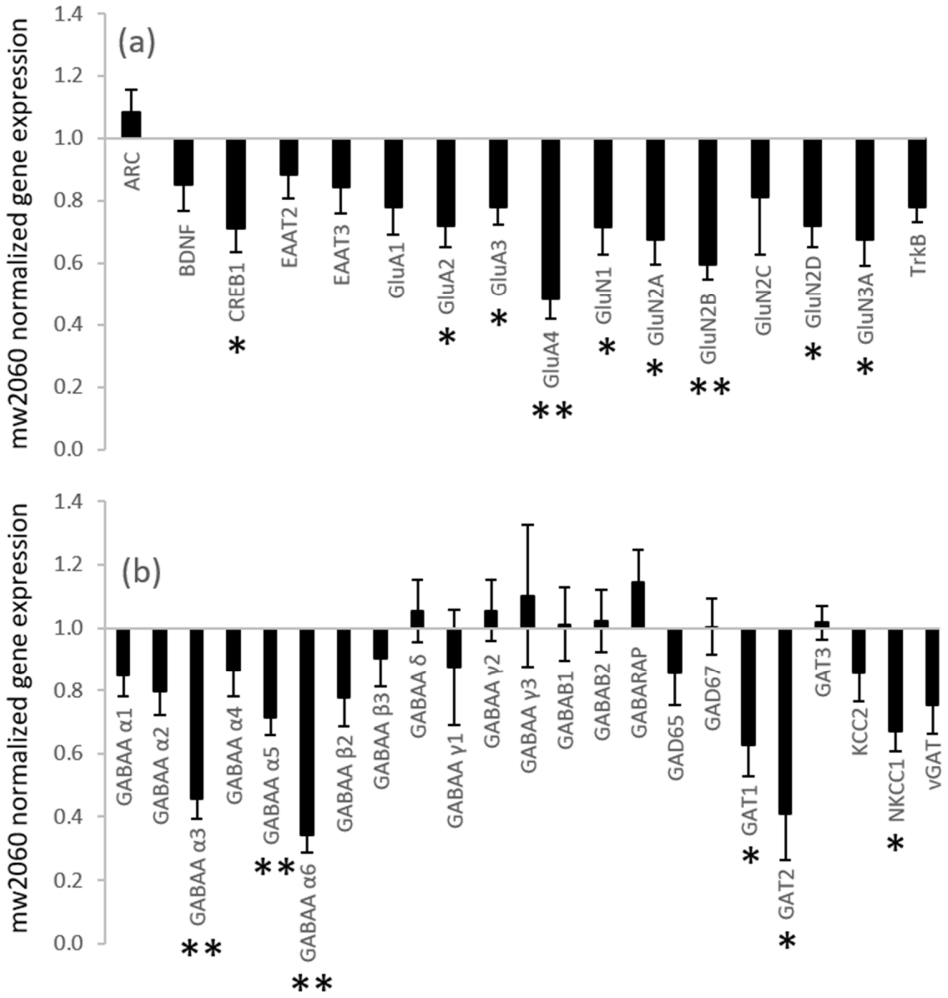
(a)
mw2060 normalized gene expression
1.4
1.2
1.0
0.8
0.6
0.4
0.2
0.0
ARC
BDNF
CREB1
EAAT2
EAAT3
GluA1
GluA2
GluA3
GluA4
GluN1
GluN2A
GluN2B
GluN2C
GluN2D
GluN3A
TrkB
(b)
mw2060 normalized gene expression
GABAA α1
GABAA α2
GABAA α3
GABAA α4
GABAA α5
GABAA α6
GABAA β2
GABAA β3
GABAA δ
GABAA γ1
GABAA γ2
GABAA γ3
GABAB1
GABAB2
GABARAP
GAD65
GAD67
GAT1
GAT2
GAT3
KCC2
NKCC1
vGAT

Figure 4.

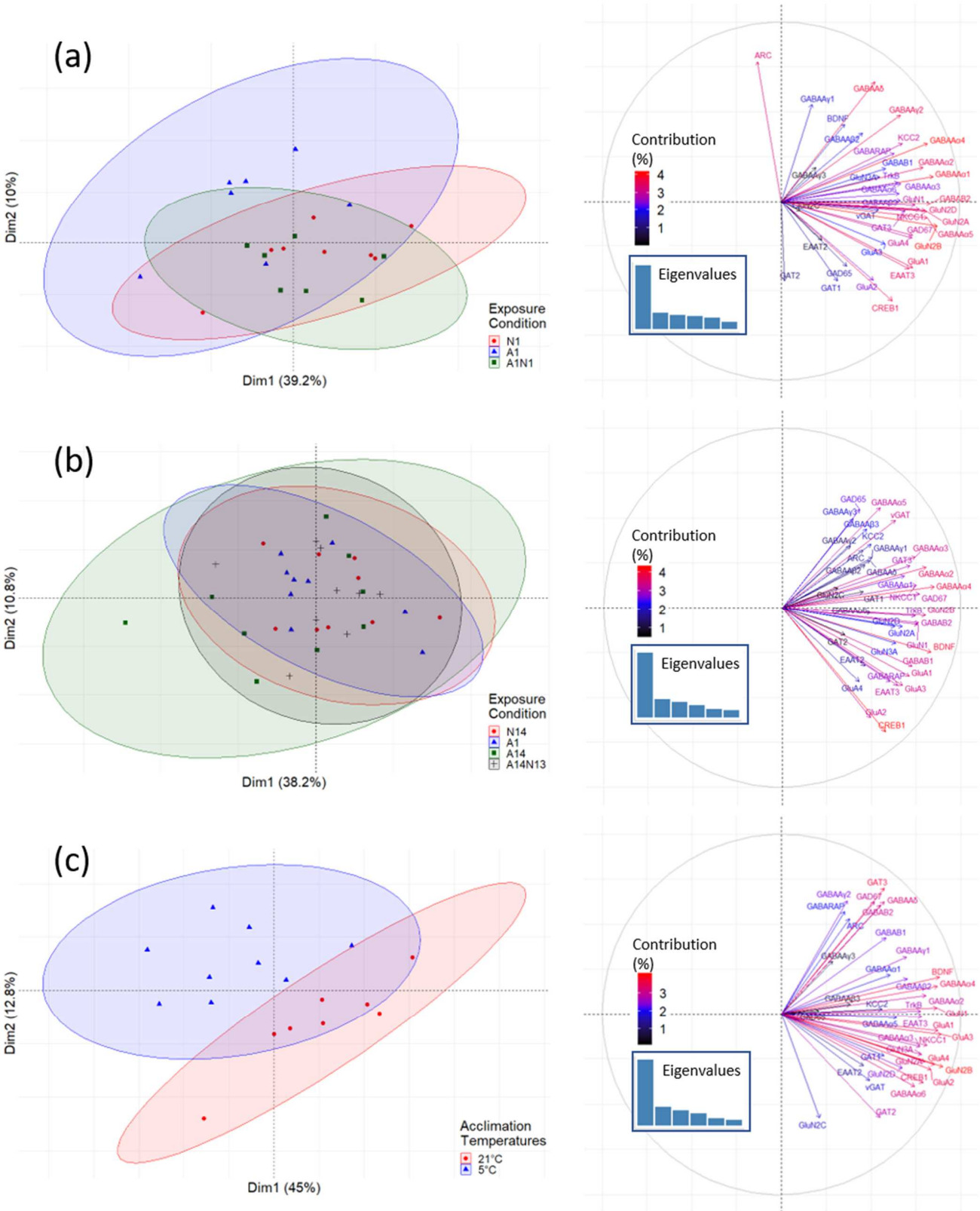
(a)
Dim2 (10%)
Dim1 (39.2%)
Exposure Condition
N1
A1
A1N1
Contribution (%)
4
3
2
1
Eigenvalues
ARC
GABAAδ
GABAAγ1
GABAAγ2
BDNF
KCC2
GABAAα4
GABARAP
GABAB1
GABAAα2
GABAAγ3
TrkB
GABAAα1
GABAAα3
GluN1
GABAB2
GluN2D
vGAT
GluN2A
GAT3
GAD67
GABAAα5
EAAT2
GluA4
GluN2B
GluA3
GluA1
GAT2
GAD65
EAAT3
GAT1
GluA2
CREB1
(b)
Dim2 (10.8%)
Dim1 (38.2%)
Exposure Condition
N14
A1
A14
A14N13
Contribution (%)
4
3
2
1
Eigenvalues
GAD65
GABAAα5
GABAAγ3
vGAT
GABAAβ3
KCC2
GABAAγ2
GABAAγ1
GABAAα3
ARC
GAT3
GABAAβ2
GABAAδ
GABAAα2
GABAAα1
GABAAα4
GluN2C
GAT1
NKCC1
GAD67
TrkB
GluN2D
GABAB2
GluN2A
GAT2
GluN1
BDNF
GluN3A
EAAT2
GABAB1
GABARAP
GluA1
GluA4
EAAT3
GluA3
GluA2
CREB1
(c)
Dim2 (12.8%)
Dim1 (45%)
Acclimation Temperatures
21°C
5°C
Contribution (%)
3
2
1
Eigenvalues
GAT3
GABAAγ2
GAD67
GABARAP
GABAAδ
GABAB2
ARC
GABAB1
GABAAγ3
GABAAγ1
GABAAα1
BDNF
GABAAβ2
GABAAα4
GABAAβ3
KCC2
TrkB
GABAAα2
GluN1
GABAAα5
EAAT3
GluA1
GABAAα3
NKCC1
GluA3
GAT1
GluN2C
GluA4
EAAT2
GluN2D
CREB1
GluN2B
vGAT
GluA2
GABAAα6
GAT2
GluN2C

Figure 5.

Table 1. The gene associated with excitatory and inhibitory neurotransmission that were cloned, their encoded protein and the properties of the primers utilized to quantify their expression by real-time RT-PCR.

	Gene	Encoded Protein	Accession #		Sequence	Priming Efficiency	Quantification Cycle	Amplicon Length
	mw2060	n/a	**DQ075244**	F	GTGCTGACCATCCGAG	1.88 ±0.02	22.1 ±0.7	235
				R	GCTTGTCCGGTATAACT			
	Arc	ARC	**MF872163**	F	ACCAGGGATGCCATCAAAC	1.89 ±0.02	28.3 ±0.8	81
				R	TCTCTTACGCCAGAGGAACTC			
	Bdnf	BDNF	**MF872164**	F	TGAGTGGGTAACAGCAGCAG	1.89 ±0.01	29.4 ±0.8	157
				R	CCTGCAACCCTCTTTTGTGT			
	Creb1	CREB1	**MF872166**	F	GAGTACAGGGCCTTCAGACG	1.87 ±0.02	28.6 ±0.8	172
				R	GCTGTGCGAATCTGGTAGGT			
	Slc1a2	EAAT2	**MF872161**	F	CCCAGGAAATCCAAAACTCA	1.87 ±0.02	24.9 ±0.8	166
				R	GGGCACCAGCACTTTCTTAG			
	Slc1a1	EAAT3	**MF872162**	F	TAAACGTCCTTGGAGATGCC	1.88 ±0.02	26.6 ±1.2	154
				R	TTCTTGGTCTCCGGTTCATC			
E	*Gria1*	GluA1	**MF872157**	F	GAAGGGGTCTGCACTGAGAG	1.90 ±0.02	26.1 ±0.7	183
X				R	ATATAGAAAACCCCGGCCAC			
C	*Gria2*	GluA2	**MF872158**	F	GAGAAGACCAGTGCCCTCAG	1.88 ±0.01	25.6 ±0.9	144
I				R	CTTTGCCACCTTCATTCGTT			
T	*Gria3*	GluA3	**MF872159**	F	CCAAGGTCTCTCTCAGGACG	1.89 ±0.02	25.6 ±0.8	143
A				R	GCCAGATCCTCTGCACTTTC			
T	*Gria4*	GluA4	**MF872160**	F	CGAGTTTGGCATCTTCAACA	1.85 ±0.02	33.5 ±1.2	196
O				R	TTCTATGGGCGAGACCATTC			
R	*Grin1*	GluN1	**MF872151**	F	ACTCGTTCATGCAGCCTTTC	1.88 ±0.02	22.8 ±0.9	238
Y				R	ATACGAGCAGAGAAGCTCCG			
	Grin2a	GluN2A	**MF872152**	F	CATTCTTGATGAAGCCCGTT	1.91 ±0.02	27.6 ±1.2	196
				R	TGCAGCTGTGCTGATAATCC			
	Grin2b	GluN2B	**MF872153**	F	AGAAGATCAATGGGACGTGG	1.87 ±0.02	25.9 ±0.9	206
				R	CATCACCCATACGTCAGCAC			
	Grin2c	GluN2C	**MF872154**	F	CCATGGTGGTGATCTCACTG	1.78 ±0.04	36.0 ±1.1	172
				R	ACAAAGGGCCTCTCTTCGAG			
	Grin2d	GluN2D	**MF872155**	F	CAGCACGGAGAAGAACATACG	1.87 ±0.02	31.0 ±1.0	101
				R	ACTTCAGGTGCTGCAGGG			
	Grin3a	GluN3A	**MF872156**	F	CAGGTCTTGTGGGTGACCTT	1.89 ±0.02	28.2 ±1.0	153
				R	GAGCGGCTGTATCTCTGGTC			
	Ntrk2	TrkB	**MF872165**	F	AATGCTCGGAAAGACTTCCA	1.86 ±0.02	26.0 ±0.8	223
				R	CATCTGGGACTGGGTCAACT			
	Gabra1	$GABA_A$ α1	**MF872167**	F	CCAGCAAGATTTGGACACCT	1.90 ±0.01	23.8 ±0.7	233
				R	CACAACCTCCGCTCTGGTAT			
	Gabra2	$GABA_A$ α2	**MF872168**	F	CCGGATGGCTCTAGATTGAA	1.89 ±0.03	25.5 ±0.7	160
				R	ATGCAGGGGGAGGTAAGTCT			
	Gabra3	$GABA_A$ α3	**MF872169**	F	CATGACAACACCCAACAAGC	1.86 ±0.02	27.5 ±0.8	218
				R	CTTTGCCCACTTCCACTGAT			
	Gabra4	$GABA_A$ α4	**MF872170**	F	GCCATGGCACAGTCAGAG	1.85 ±0.02	26.0 ±0.7	155
				R	TCTGATACATTGAGGCGACTG			
	Gabra5	$GABA_A$ α5	**MF872171**	F	GCGCCCAGGACTGGGAGAGA	1.91 ±0.02	27.1 ±0.7	164
				R	GGAGGCGTTGCATCGGTCCTTT			
	Gabra6	$GABA_A$ α6	**MF872172**	F	ACTGCCATGGATTGGTTCAT	1.88 ±0.02	31.5 ±1.0	157
				R	TTGCTGCTGATAGTGCTGCT			
	Gabrb2	$GABA_A$ β2	**MF872174**	F	CTCCTGGGTTTCATTCTGGA	1.91 ±0.02	24.2 ±0.8	182
				R	GGGCCATAAAAACGAAGACA			
	Gabrb3	$GABA_A$ β3	**MF872175**	F	TGTCTTCGCCACAGGTGCGT	1.91 ±0.02	26.1 ±0.8	165
				R	AGGGCAACTCTTGCTGCTGATGC			
I	*Gabrd*	$GABA_A$ δ	**MF872176**	F	ATGTCGTGGGTTTCCTTCTG	1.89 ±0.01	27.0 ±0.7	198
N				R	TGCATATTCCACCAGAGCAG			
H	*Gabrg1*	$GABA_A$ γ1	**MF872177**	F	AAAGAGAAGTCTTCAAAACACAAGC	1.85 ±0.02	32.4 ±1.0	151
I				R	TGGTACAGTCTTTCCCTTCCAG			
B	*Gabrg2*	$GABA_A$ γ2	**MF872178**	F	ACATGGTTGGGAAGATCTGG	1.88 ±0.02	24.8 ±0.7	199
I				R	AGCGGACAGGAATGTTCATC			
T	*Gabrg3*	$GABA_A$ γ3	**MF872179**	F	TGGAAACCTCTGCAGGTGA	1.83 ±0.04	30.7 ±1.3	155

O				R	TGCTGGTGTGGCATCTTTT			
R	*Gabbr1*	$GABA_{B1}$	**MF872180**	F	CTGGCATCGAGATCACCTTC	1.85 ±0.03	23.3 ±0.8	181
Y				R	ATCAGGAACCAGACGTACCG			
	Gabbr2	$GABA_{B2}$	**MF872181**	F	TATGCCTACAAAGGGCTGCT	1.92 ±0.02	25.4 ±0.7	166
				R	GATCCCGAGTGAGGAATGAA			
	Slc6a1	GAT1	**MF872182**	F	GCTTGGAATTGACAGCCAGT	1.90 ±0.02	24.1 ±1.3	207
				R	AGGCTCATTCCACTTGCAGA			
	Slc6a13	GAT2	**MF872183**	F	GCTGGCTTTGCAATCTTTTC	1.89 ±0.02	28.2 ±1.7	245
				R	ATGGTGGGGTACATGTCGAT			
	Slc6a11	GAT3	**MF872184**	F	AGCCTTGTGACAGCTGTGGTGG	1.92 ±0.01	25.9 ±0.7	178
				R	GGCACATCCCACTGGCTGCAT			
	Slc32a1	vGAT	**MF872185**	F	GTGGTCAGTGGGAACCTGAT	1.89 ±0.02	26.6 ±0.7	158
				R	AAGTGGGCTAAGGTGCAGAG			
	Gad2	GAD65	**MF872186**	F	GACTTGAAACCCCCACAAGA	1.82 ±0.02	27.9 ±1.2	207
				R	CACATCAGCCAAAGCTTGAA			
	Gad1	GAD67	**MF872187**	F	GGTTGATGTGGAAGGCAAAGGGT	1.92 ±0.01	24.5 ±0.8	138
				R	TGTGTTCAGGCTCTCCATCAAAAACCA			
	Gabarap	GABARAP	**MF872188**	F	CTGGTCCCATCAGACCTCAC	1.93 ±0.02	22.8 ±0.6	108
				R	GGGGATGACATTGTTGACG			
	Slc12a2	NKCC1	**MF872189**	F	ACGTCCTGCTTTGGTTCATC	1.90 ±0.02	28.2 ±0.8	204
				R	TGTCCCCCATCTCTCAAATC			
	Slc12a5	KCC2	**MF872190**	F	CCGAAAGCATCAAGGACTTC	1.80 ±0.03	26.0 ±0.9	151
				R	CCTGGCATGTTCAGCAAGA			

F, forward primer; R, reverse primer. n/a, not applicable. Values are means ±SD.

Table 2. Exposure conditions and telencephalon total RNA content per mg tissue.

Temperature (°C)	Oxygenation state	N	Total RNA Content (ng mg^{-1} tissue)
21	N1	8	728 ±81
21	A1	7	682 ±113
21	A1N1	7	667 ±158
5	N14	9	738 ±100
5	A1	9	691 ±126
5	A14	9	632 ±182
5	A14N13	10	773 ±95

State of oxygenation (N: Normoxia, A: Anoxia) are followed by the number of days of exposure.
Total RNA data are from Stecyk et al.(Stecyk et al., 2012). Values are means ±SD.

Table 3. Expression of genes involved in excitatory and inhibitory neurotransmission pathways in *Trachemys scripta* telencephalon at 21°C in normoxia, anoxia and after reoxygenation.

	Gene	Encoded Protein	N1	A1	A1N1	Sig. Diff.
	Arc	ARC	1 ±0.06 [b]	2.05 ±0.20 [a]	1.01 ±0.06 [b]	***
	Bdnf	BDNF	1 ±0.11 [ab]	1.17 ±0.09 [a]	0.80 ±0.09 [b]	*
	Creb1	CREB1	1 ±0.07 [ab]	0.88 ±0.07 [b]	1.24 ±0.07 [a]	**
E	*Slc1a2*	EAAT2	1 ±0.03	0.88 ±0.06	0.94 ±0.09	NS
X	*Slc1a1*	EAAT3	1 ±0.10 [a]	0.73 ±0.06 [b]	0.95 ±0.07 [ab]	*
C	*Gria1*	GluA1	1 ±0.09 [ab]	0.78 ±0.05 [b]	1.10 ±0.10 [a]	*
I	*Gria2*	GluA2	1 ±0.08	0.90 ±0.12	1.02 ±0.11	NS
T	*Gria3*	GluA3	1 ±0.07	0.90 ±0.08	0.89 ±0.04	NS
A	*Gria4*	GluA4	1 ±0.16	0.77 ±0.10	0.88 ±0.06	NS
T	*Grin1*	GluN1	1 ±0.11	0.88 ±0.07	1.03 ±0.10	NS
O	*Grin2a*	GluN2A	1 ±0.09	0.89 ±0.10	0.96 ±0.06	NS
R	*Grin2b*	GluN2B	1 ±0.08	0.78 ±0.05	0.96 ±0.10	NS
Y	*Grin2c*	GluN2C	1 ±0.14	0.67 ±0.13	0.64 ±0.10	NS
	Grin2d	GluN2D	1 ±0.09	0.80 ±0.07	0.90 ±0.05	NS
	Grin3a	GluN3A	1 ±0.10	0.77 ±0.05	0.80 ±0.08	NS
	Ntrk2	TrkB	1 ±0.10	0.87 ±0.05	1.00 ±0.10	NS
	Gabra1	$GABA_A$ α1	1 ±0.07	0.82 ±0.07	0.94 ±0.08	NS
	Gabra2	$GABA_A$ α2	1 ±0.08	0.83 ±0.09	0.79 ±0.08	NS
	Gabra3	$GABA_A$ α3	1 ±0.18	0.63 ±0.07	0.85 ±0.09	NS
	Gabra4	$GABA_A$ α4	1 ±0.08	0.86 ±0.10	0.95 ±0.09	NS
	Gabra5	$GABA_A$ α5	1 ±0.08 [a]	0.59 ±0.10 [b]	0.78 ±0.107 [ab]	*
	Gabra6	$GABA_A$ α6	1 ±0.12	0.60 ±0.08	0.92 ±0.20	NS
I	*Gabrb2*	$GABA_A$ β2	1 ±0.12	1.00 ±0.17	0.85 ±0.09	NS
N	*Gabrb3*	$GABA_A$ β3	1 ±0.07	0.78 ±0.09	0.86 ±0.08	NS
H	*Gabrd*	$GABA_A$ δ	1 ±0.13	1.04 ±0.17	0.81 ±0.06	NS
I	*Gabrg1*	$GABA_A$ γ1	1 ±0.20	0.95 ±0.08	0.75 ±0.15	NS
B	*Gabrg2*	$GABA_A$ γ2	1 ±0.07	0.94 ±0.07	0.96 ±0.07	NS
I	*Gabrg3*	$GABA_A$ γ3	1 ±0.17	1.00 ±0.12	1.27 ±0.14	NS
T	*Gabbr1*	$GABA_{B1}$	1 ±0.13	0.92 ±0.10	1.13 ±0.14	NS
O	*Gabbr2*	$GABA_{B2}$	1 ±0.11	0.79 ±0.06	1.13 ±0.10	NS
R	*Gabarap*	GABARAP	1 ±0.09	1.04 ±0.12	1.21 ±0.15	NS
Y	*Gad2*	GAD65	1 ±0.15	0.75 ±0.09	1.16 ±0.20	NS
	Gad1	GAD67	1 ±0.10	0.80 ±0.07	1.14 ±0.12	NS
	Slc6a1	GAT1	1 ±0.13	0.66 ±0.12	1.11 ±0.23	NS
	Slc6a13	GAT2	1 ±0.14	0.68 ±0.17	1.00 ±0.21	NS
	Slc6a11	GAT3	1 ±0.10	0.86 ±0.06	1.12 ±0.12	NS
	Slc12a5	KCC2	1 ±0.11	0.92 ±0.15	0.92 ±0.11	NS
	Slc12a2	NKCC1	1 ±0.11	0.70 ±0.11	0.79 ±0.06	NS
	Slc32a1	vGAT	1 ±0.09	0.75 ±0.12	0.88 ±0.09	NS

For abbreviations of oxygenation state see Table 2. Data sets are normalized to the external RNA control mw2060 and referenced to the control normoxic turtles. Statistical analysis: one-way ANOVA (level of significance: NS non-significant, * $P < 0.05$, ** $P < 0.01$,

*** $P < 0.001$; *P*-values and *F*-ratios are provided in Table S1) and Tukey HSD *post hoc* test (dissimilar letters indicate statistically significant differences among exposure groups for each gene). Values are means ±SEM. N=7-8 per exposure group.

051 Table 4. Gene-family profiles per exposure condition (%).

	Gene(s)	Encoded Protein(s)	21 °C				5 °C					21N1-5N1
			N1	A1	A1N1	Sig.	N1	A1	A14	A14N13	Sig.	Sig.
	Slc1a2	EAAT2	74.4 ±2.1	77.2 ±2.1	73.3 ±2.3	NS	74.9 ±1.7	74.2 ±2.1	71.3 ±1.7	72.2 ±1.1	NS	NS
	Slc1a1	EAAT3	25.6 ±2.1	22.8 ±2.1	26.7 ±2.3	NS	25.1 ±1.7	25.8 ±2.1	28.7 ±1.7	27.8 ±1.1	NS	NS
E	*Gria1*	GluA1	24.3 ±1.2	23.0 ±1.9	26.0 ±1.2	NS	24.8 ±0.9 ^{ab}	24.7 ±1.1 ^{ab}	21.8 ±0.6 ^{b}	28.6 ±2.4 ^{a}	*	NS
X	*Gria2*	GluA2	40.5 ±0.9	41.5 ±1.8	41.8 ±2.2	NS	38.2 ±0.5 ^{ab}	40.1 ±0.9 ^{ab}	42.5 ±0.9 ^{a}	36.5 ±2.0 ^{b}	*	*
C	*Gria3*	GluA3	34.6 ±1.1	35.0 ±0.4	31.6 ±1.6	NS	36.6 ±1.2	34.7 ±0.7	35.2 ±0.8	34.3 ±1.1	NS	NS
I	*Gria4*	GluA4	0.7 ±0.1	0.6 ±0.1	0.6 ±0.0	NS	0.4 ±0.0	0.5 ±0.1	0.5 ±0.0	0.5 ±0.0	NS	*
T	*Grin1*	GluN1	77.2 ±1.2	79.2 ±0.9	78.9 ±1.7	NS	79.8 ±1.6 ^{a}	80.4 ±0.8 ^{a}	82.8 ±0.8 ^{a}	83.7 ±0.8 ^{a}	*	NS
A	*Grin2a,b,c,d*	GluN2A,B,C,D	19.4 ±0.9	17.9 ±0.8	18.7 ±1.6	NS	17.2 ±1.2 ^{a}	16.9 ±0.8 ^{a}	14.6 ±0.8 ^{a}	14.0 ±0.6 ^{a}	*	NS
T	*Grin3a*	GluN3A	3.4 ±0.5	2.9 ±0.3	2.4 ±0.24	NS	3.0 ±0.4	2.7 ±0.2	2.6 ±0.2	2.4 ±0.2	NS	NS
O	*Grin2a*	GluN2A	16.9 ±0.5	18.4 ±1.1	16.7 ±0.8	NS	18.2 ±1.2	19.0 ±1.2	17.7 ±0.9	16.6 ±1.3	NS	NS
R	*Grin2b*	GluN2B	79.0 ±0.8	77.6 ±1.1	79.6 ±0.8	NS	79.9 ±1.1	76.3 ±1.1	77 ±0.8	78.0 ±1.2	NS	NS
Y	*Grin2c*	GluN2C	1.1 ±0.2	0.8 ±0.2	0.7 ±0.1	NS	1.3 ±0.3	1.3 ±0.3	1.2 ±0.1	1.3 ±0.4	NS	NS
	Grin2d	GluN2D	3.0 ±0.1	3.1 ±0.2	3.0 ±0.1	NS	3.7 ±0.2	3.5 ±0.2	4.1 ±0.3	4.0 ±0.2	NS	*
	Gabra1	$GABA_A$ α1	41.9 ±1.1	43.7 ±1.3	44.0 ±1.5	NS	45.0 ±2.1	48.4 ±2.1	47.3 ±1.0	45.7 ±1.1	NS	NS
	Gabra2	$GABA_A$ α2	19.3 ±0.4 ^{ab}	19.9 ±0.8 ^{a}	17.0 ±0.8 ^{b}	*	21.0 ±1.7	17.8 ±0.7	18.4 ±0.5	17.8 ±0.9	NS	NS
	Gabra3	$GABA_A$ α3	10.6 ±1.3	8.7 ±0.2	10.4 ±0.9	NS	6.8 ±0.7	7.0 ±0.8	5.5 ±0.3	6.6 ±0.5	NS	**
	Gabra4	$GABA_A$ α4	21.8 ±0.7	23.1 ±1.1	23.0 ±1.1	NS	26.1 ±2.7	21.2 ±0.7	23.9 ±1.0	24.0 ±1.2	NS	NS
I	*Gabra5*	$GABA_A$ α5	5.8 ±0.3 ^{a}	4.1 ±0.3 ^{b}	4.9 ±0.4 ^{ab}	**	5.8 ±0.6	5.2 ±0.6	4.6 ±0.5	5.5 ±0.4	NS	NS
N	*Gabra6*	$GABA_A$ α6	0.7 ±0.1	0.5 ±0.1	0.7 ±0.1	NS	0.3 ±0.0	0.4 ±0.0	0.3 ±0.1	0.4 ±0.1	NS	***
H	*Gabrb2*	$GABA_A$ β2	78.5 ±1.2	82.2 ±1.3	78.9 ±1.3	NS	76.2 ±1.4	74.9 ±1.2	75.8 ±1.8	72.4 ±2.0	NS	NS
I	*Gabrb3*	$GABA_A$ β3	21.5 ±1.2	17.8 ±1.3	21.1 ±1.3	NS	23.8 ±1.4	25.1 ±1.2	24.2 ±1.8	27.6 ±2.0	NS	NS
B	*Gabrg1*	$GABA_A$ γ1	1.6 ±0.3	1.6 ±0.1	1.3 ±0.3	NS	1.4 ±0.3	1.8 ±0.3	1.2 ±0.2	1.4 ±0.2	NS	NS
I	*Gabrg2*	$GABA_A$ γ2	91.8 ±1.2	91.4 ±0.6	90.3 ±0.5	NS	92.1 ±1.2	90.0 ±1.3	93.0 ±0.4	91.4 ±0.4	NS	NS
T	*Gabrg3*	$GABA_A$ γ3	6.6 ±1.1	7.0 ±0.6	8.4 ±0.5	NS	6.6 ±1.1	8.2 ±1.1	5.8 ±0.3	7.3 ±0.4	NS	NS
O	*Gabbr1*	$GABA_B$1	90.4 ±0.7	91.6 ±0.3	90.2 ±0.8	NS	90.2 ±0.4	88.7 ±0.7	89.0 ±0.5	89.4 ±0.8	NS	NS
R	*Gabbr2*	$GABA_B$2	9.6 ±0.7	8.4 ±0.3	9.8 ±0.8	NS	9.8 ±0.4	11.3 ±0.7	11.0 ±0.5	10.6 ±0.8	NS	NS
Y	*Gabrd*	$GABA_A$ δ	20.5 ±1.6	21.9 ±2.0	18.6 ±1.2	NS	21.3 ±1.4	20.4 ±1.0	19.5 ±1.5	17.8 ±0.7	NS	NS
	Gabrg2	$GABA_A$ γ2	79.5 ±1.6	78.1 ±2.0	81.4 ±1.2	NS	78.7 ±1.4	79.6 ±1.0	80.5 ±1.5	82.2 ±0.7	NS	NS
	Gad2	GAD_{65}	34.7 ±2.7	33.6 ±2.1	34.5 ±2.4	NS	31.4 ±2.2	36.3 ±3.0	27.0 ±2.9	36.2 ±4.1	NS	NS
	Gad1	GAD_{67}	65.3 ±2.7	66.4 ±2.1	65.5 ±2.4	NS	68.6 ±2.2	63.7 ±3.0	73.0 ±2.9	63.8 ±4.1	NS	NS
	Slc6a1	GAT1	73.7 ±2.4	69.2 ±2.6	72.7 ±4.1	NS	67.7 ±2.9	76.8 ±1.4	75.8 ±2.6	75.0 ±2.9	NS	NS
	Slc6a13	GAT2	9.4 ±1.5	8.4 ±1.7	8.4 ±2.0	NS	4.8 ±1.6	5.7 ±1.0	7.1 ±1.3	7.9 ±1.3	NS	*
	Slc6a11	GAT3	16.9 ±1.9	22.4 ±3.2	18.9 ±2.8	NS	27.6 ±3.2 ^{a}	17.5 ^{ab} ±1.6	17.1 ±2.4 ^{b}	17.1 ±3.4 ^{b}	*	*

052 For abbreviations of oxygenation state see Table 2. Statistical analysis: one-way ANOVA (level of significance: NS non-significant, *
053 $P < 0.05$, ** $P < 0.01$, *** $P < 0.001$ *P*-values, *F*- and *t*-ratios are provided in Table S2) and Tukey HSD *post hoc* test (dissimilar
054 letters indicate statistically significant differences among exposure groups for each gene). Values are means ±SEM. N=7-10 per
055 exposure group.

056

Table 5. Expression of genes involved in excitatory and inhibitory neurotransmission pathways in *Trachemys scripta* telencephalon at 5°C in normoxia, anoxia and after reoxygenation.

	Gene	Encoded Protein	N1	A1	A14	A14N13	Sig. Diff.
	Arc	ARC	1 ±0.07 [a]	0.84 ±0.10 [ab]	0.69 ±0.6 [b]	1.22 ±0.13 [a]	**
	Bdnf	BDNF	1 ±0.10	0.97 ±0.10	0.84 ±0.09	0.93 ±0.11	NS
	Creb1	CREB1	1 ±0.11	1.03 ±0.10	0.89 ±0.06	1.00 ±0.08	NS
E	*Slc1a2*	EAAT2	1 ±0.09	0.95 ±0.14	0.70 ±0.05	0.82 ±0.05	NS
X	*Slc1a1*	EAAT3	1 ±0.10	0.93 ±0.09	0.84 ±0.07	0.94 ±0.05	NS
C	*Gria1*	GluA1	1 ±0.11	0.95 ±0.11	0.75 ±0.05	0.98 ±0.06	NS
I	*Gria2*	GluA2	1 ±0.09	0.99 ±0.11	0.94 ±0.05	0.87 ±0.11	NS
T	*Gria3*	GluA3	1 ±0.07	0.93 ±0.08	0.85 ±0.04	0.87 ±0.08	NS
A	*Gria4*	GluA4	1 ±0.13	0.99 ±0.12	1.01 ±0.11	1.02 ±0.14	NS
T	*Grin1*	GluN1	1 ±0.12	1.05 ±0.12	1.02 ±0.11	1.30 ±0.09	NS
O	*Grin2a*	GluN2A	1 ±0.12	1.06 ±0.09	0.86 ±0.08	0.92 ±0.09	NS
R	*Grin2b*	GluN2B	1 ±0.09	1.06 ±0.12	0.84 ±0.08	1.05 ±0.10	NS
Y	*Grin2c*	GluN2C	1 ±0.23	1.05 ±0.28	0.77 ±0.09	1.00 ±0.25	NS
	Grin2d	GluN2D	1 ±0.09	1.00 ±0.09	0.94 ±0.12	1.15 ±0.12	NS
	Grin3a	GluN3A	1 ±0.13	0.96 ±0.09	0.85 ±0.12	0.95 ±0.10	NS
	Ntrk2	TrkB	1 ±0.06	1.06 ±0.10	0.94 ±0.09	1.04 ±0.11	NS
	Gabra1	$GABA_A$ α1	1 ±0.08	1.10 ±0.11	0.96 ±0.13	0.93 ±0.10	NS
	Gabra2	$GABA_A$ α2	1 ±0.09	0.93 ±0.08	0.86 ±0.12	0.82 ±0.07	NS
	Gabra3	$GABA_A$ α3	1 ±0.14	1.11 ±0.13	0.77 ±0.09	0.92 ±0.09	NS
	Gabra4	$GABA_A$ α4	1 ±0.10	0.90 ±0.06	0.92 ±0.13	0.94 ±0.11	NS
	Gabra5	$GABA_A$ α5	1 ±0.08	0.96 ±0.06	0.86 ±0.19	0.95 ±0.10	NS
	Gabra6	$GABA_A$ α6	1 ±0.17	1.20 ±0.18	0.99 ±0.26	1.18 ±0.17	NS
I	*Gabrb2*	$GABA_A$ β2	1 ±0.12	0.84 ±0.04	0.81 ±0.10	0.68 ±0.07	NS
N	*Gabrb3*	$GABA_A$ β3	1 ±0.10	0.92 ±0.06	0.87 ±0.14	0.84 ±0.10	NS
H	*Gabrd*	$GABA_A$ δ	1 ±0.09 [a]	0.74 ±0.04 [ab]	0.75 ±0.08 [ab]	0.70 ±0.04 [b]	*
I	*Gabrg1*	$GABA_A$ γ1	1 ±0.21	1.04 ±0.15	0.76 ±0.11	0.90 ±0.14	NS
B	*Gabrg2*	$GABA_A$ γ2	1 ±0.09	0.77 ±0.03	0.88 ±0.13	0.86 ±0.05	NS
I	*Gabrg3*	$GABA_A$ γ3	1 ±0.20	0.95 ±0.14	0.74 ±0.12	0.92 ±0.07	NS
T	*Gabbr1*	$GABA_{B1}$	1 ±0.12	0.71 ±0.05	0.77 ±0.09	0.82 ±0.07	NS
O	*Gabbr2*	$GABA_{B2}$	1 ±0.10	0.87 ±0.08	0.90 ±0.11	0.89 ±0.07	NS
R	*Gabarap*	GABARAP	1 ±0.09 [a]	0.69 ±0.07 [b]	0.86 ±0.08 [ab]	0.88 ±0.05 [ab]	*
Y	*Gad2*	GAD65	1 ±0.12	1.12 ±0.14	0.68 ±0.11	1.20 ±0.21	NS
	Gad1	GAD67	1 ±0.09	0.91 ±0.07	0.82 ±0.08	0.91 ±0.08	NS
	Slc6a1	GAT1	1 ±0.16	1.51 ±0.22	1.40 ±0.27	1.49 ±0.21	NS
	Slc6a13	GAT2	1 ±1.36	1.57 ±0.34	1.74 ±0.45	1.97 ±0.27	NS
	Slc6a11	GAT3	1 ±0.05	0.89 ±0.06	0.76 ±0.07	0.82 ±0.07	NS
	Slc12a5	KCC2	1 ±0.11	0.74 ±0.12	0.77 ±0.10	0.98 ±0.10	NS
	Slc12a2	NKCC1	1 ±0.09	1.11 ±0.10	0.99 ±0.15	1.08 ±0.16	NS
	Slc32a1	vGAT	1 ±0.12	1.18 ±0.12	0.80 ±0.12	1.05 ±0.09	NS

For abbreviations of oxygenation state see Table 2. Data sets are normalized to the external RNA control mw2060 and referenced to the control normoxic turtles. Statistical analysis: one-way ANOVA (level of significance: NS non-significant, * $P < 0.05$, ** $P < 0.01$, *** $P < 0.001$; *P*-values and *F*-ratios are provided in Table S3) and Tukey HSD *post hoc* test (dissimilar letters indicate statistically significant differences among exposure groups for each gene). Values are means ±SEM. N=9-10 per exposure group.

Table 6. Results (*P* values) of the pairwise one-way permutational multivariate analysis of variance (PERMANOVA) utilized to assess differences in the pattern of gene expression of the 39 target genes among the seven exposure conditions.

Exposure condition		21°C			5°C			
		N1	A1	A1N1	N14	A1	A14	A14N13
21°C	N1	-	**0.0101**	0.4239	**0.0007**	**0.0024**	**0.0005**	**0.0004**
	A1	**0.0101**	-	**0.0225**	**0.0456**	**0.0383**	**0.0181**	**0.0138**
	A1N1	0.4239	**0.0225**	-	**0.0038**	**0.0116**	**0.0032**	**0.0016**
5°C	N14	**0.0007**	**0.0456**	**0.0038**	-	0.2727	0.1093	0.0692
	A1	**0.0024**	**0.0383**	**0.0116**	0.2727	-	0.2574	0.5660
	A14	**0.0005**	**0.0181**	**0.0032**	0.1093	0.2574	-	0.2276
	A14N13	**0.0004**	**0.0138**	**0.0016**	0.0692	0.5660	0.2276	-

For abbreviations of oxygenation state see Table 2.
Bold text highlights statistically significant differences.
Red shading highlights pairwise comparisions between normoxia, anoxia and reoxygenation at 21°C.
Blue shading highlights pairwise comparisions between normoxia, anoxia and reoxygenation at 5°C.
For corresponding *F*-ratios see Table S5.